MINISTRY OF TECHNOLOGY

AERONAUTICAL RESEARCH COUNCIL

CURRENT PAPERS

The Role of Heat Conduction in Leading Edge Heating Theory and Experiment

By

T. Nonweiler, B.Sc., Ph.D.,

H. Y. Wong, B.Sc., Ph.D., D.I.C.,

S. R. Aggarwal, B.Sc.,

University of Glasgow Dept. of Aeronautics and Fluid Mechanics

THE ROLE OF HEAT CONDUCTION IN LEADING EDGE HEATING
THEORY AND EXPERIMENT

by

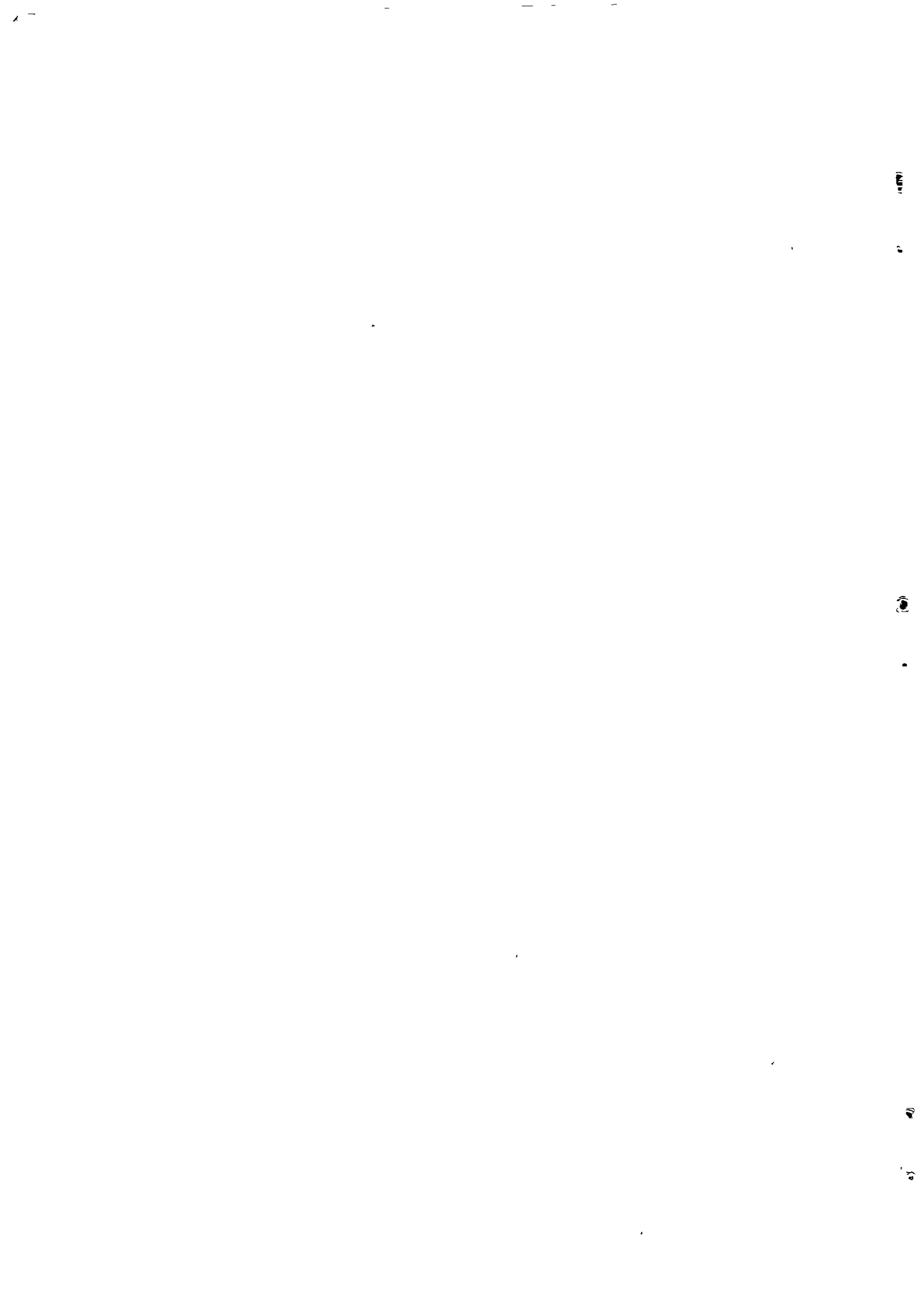T. Nonweiler, B.Sc., Ph.D.,

H. Y. Wong, B.Sc., Ph.D., D.I.C.,

S. R. Aggarwal, B.Sc.,

University of Glasgow Dept. of Aeronautics
and Fluid Mechanics

SUMMARY

The effect of heat conduction of material on the temperature distribution in the vicinity of a wing leading edge in hypersonic flight is investigated. The theory is based on a conducting plate subjected to aerodynamic heating. It is found that the role played by the conductivity of the material and the leading edge thickness in moderating the nose temperature is very significant. Detailed discussions of the numerical solutions for various shapes of leading edge are given. An experimental technique has been developed by which a number of models representing a wing leading edge can be tested and the results thus obtained are compared with those predicted by the theory.

LIST OF CONTENTS

1. Introduction

In principle, there is no difficulty in applying a numerical process to the solution of the steady state temperature distribution within a body subjected to heat transfer, which can be implemented with the help of a digital computer. However, where the body is as complicated as the structure of an aircraft, and the heat transfer is aerodynamic in origin, the problem can well be beyond the reasonable capabilities of present day computers, unless some simplifying assumptions are introduced in setting up the problem.

One such simplification was introduced by one of the authors some time ago (ref.1,2), which sought to provide a basis for estimating the temperature close to the leading-edge of a wing in hypersonic flight, where the conduction of heat within the material of the wing can be predominant in determining the temperature reached. Interest has again been awakened in this problem (ref. 3), and with a view to using the approximation derived in this early work to study the leading edge temperature of wings of finite span, it was decided to check the numerical solutions given therein (which were achieved by slide rule methods), and to attempt to corroborate the approximation by experiment. This report is the outcome, and work on the finite wing (though not reported here) is well advanced.

Basically we have in mind that the wing is geometrically thin, and (so far as its overall aerodynamic properties are affected) "sharp-edged". As we shall see, we envisage more precisely a leading edge radius of 1 cm. or so, but not of 1 m. or thereabouts which would be necessary to alleviate the intense heat transfer rates associated with "sharp" leading edges. Metallic material concentrated in this leading edge region conducts the heat input from the boundary layer downstream, and this results in a leading edge temperature considerably less than the "thermometer" value otherwise reached.

Mathematically, the approximation consists of assuming that the thickness of the wing is infinitesimal, but that its conductivity is infinite; not to include the latter renders the problem trivial, as the temperature of the resulting plate is everywhere equal to the radiation equilibrium value. For a "conducting plate" on the other hand, the solution is non trivial, and it is believed it represents with reasonable accuracy many problems of practical interest.

Paragraph two of this report gives details of the theory, amplifying what is behind the approximation. The simplified equations for the temperature distribution can still be troublesome to solve, and we restrict ourselves here to a particular set of boundary conditions (paragraph 2.1) and make various other simplifying assumptions about the environment (paragraph 2.3). Certain similarity relations result which suggest how laboratory experiments in a relative low temperature environment may be scaled up to provide information of practical value, and vice versa. In paragraph 2.5, there is a detailed discussion of the numerical solution for various shapes of leading edge assuming a heat input proportional to $1/x^{\frac{1}{2}}$ (where x is the distance from the leading edge) and this includes a description of an optimum distribution of conducting material. Heat distributions obtained in the laboratory cannot of course include a singularity, and the effects of this are considered in paragraph 2.6.

An/

An experimental apparatus is described in paragraph 3 which employs the radiation of an electric filament heater reflected by a specially designed mirror onto a model in a vacuum chamber, to obtain a heat distribution resembling that near a leading edge of a wing. This has been used in the first case to verify the theoretical approximations - with reasonable success. It is also intended for use in its own right to investigate conditions which would still be troublesome to study theoretically.

2. The Theory of Conducting Plates

The form of the approximation is based on the supposition that the solid body is composed of highly conductive material, but is thin. In mathematical terms, it is derived by asserting that, if k_0 and t_0 are measures of the general orders of magnitude of thermal conductivity and thickness (perpendicular, say, to the plan $Z = 0$ of a cartesian axis system), then we allow (t_0/k_0) to tend to zero, with $(t_0 k_0)$ remaining finite. We note that, if Q_0 is the general magnitude of heat flux normal to the surface of the body then the change in temperature across the thickness will be of order $(Q_0 t_0/k_0)$, and the essential point of the approximation is that this is small compared with T_0 - or in other words $(Q_0 t_0/k_0 T_0)$ is a small quantity and is indeed treated as vanishingly small to justify the argument in mathematical terms.

We may then treat the temperature T within such a body as a function only of x, and the equation for steady heat conduction merely equates the rate of change of heat flux within the body per unit span in the direction of the x-axis, that is $-\frac{d}{dx}(kt\frac{dT}{dx})$, with the net rate of normal flux, which equals $(Q - \varepsilon\sigma T^4)$, where Q is the quantity of heat transferred to the top and bottom body surfaces and $\varepsilon\sigma T^4$ is that emitted from them by radiation, (here ε is the sum of the upper and lower surface emissivity, and σ is Stefan's constant). If we supposed that $(k_0 t_0)$ tended to zero with (t_0/k_0), then this would be tantamount to ignoring longitudinal (as well as transverse) heat conduction within the body; in which event, of course, we would obtain the well-known result for a non-conducting plate, that the steady state surface temperature distribution tends to the radiation equilibrium temperature. This may indeed be an adequate approximation in many practical problems. However, in relation to the heat transfer at high speeds of flight to sharp edged wings (or pointed bodies), the radiation equilibrium temperature at the leading edge (or nose) is equal to the thermometer temperature, and this may be several times larger than the general magnitude of the temperature downstream. In such a context, the heat transfer to the body may suffer unit order changes over a length of surface (ℓ, say) close to the leading edge, so that there would be local temperature gradients of order (T_0/ℓ), and consequently a longitudinal heat flux of magnitude $(k_0 t_0 T_0/\ell)$. Where longitudinal conduction becomes important, therefore, we would anticipate that this heat flux becomes comparable in magnitude to $Q_0\ell$. Conversely, if we suppose that, as $(t_0 Q_0/k_0 t_0) \rightarrow 0$,

$$1/(k_0 t_0) = O\ (T_0/Q_0\ell^2) \qquad\qquad \dots (1)$$

so that $k_0 t_0$ remains non-zero in this limit (as we have previously postulated), then longitudinal conduction may be of consequence over the distance ℓ.

These/

These assumptions can usefully be restated by defining lengths

$$\lambda = k_0 T_0 / Q_0 \quad \text{and} \quad \ell = (\lambda t_0)^{\frac{1}{2}} \qquad \ldots (2)$$

The basic assumption is then that $(t_0 / \lambda) \to 0$, and we shall consider problems in which Q_0 suffers unit order changes over the length ℓ, which remains (conceptually) finite in the limit. Although the radiation emitted will no longer equal the heat transfer to the surface in such a region, it will in general retain the same order of magnitude, so that it is reasonable to define

$$\varepsilon_0 \sigma T_0^4 = Q_0 \qquad \ldots (3)$$

and consequently in (2) we have

$$\lambda = k_0 / \varepsilon_0 \sigma T_0^3 = k_0 / (\varepsilon_0 \sigma Q_0^3)^{\frac{1}{4}} \qquad \ldots (4)$$

In practical terms, we may hope that the approximation is valid if (t_0 / λ) is 'small' compared with unity, and that the results will be of consequence if ℓ is an 'appreciable' length. The adjectives used here are necessarily vague, but it may be helpful, if not relevant as any kind of justification, to illustrate the magnitudes we are likely to be considering. It would be unlikely for instance that values of $\varepsilon_0^{1/3} T_0$ in excess of $1000^\circ K$ would be of interest in a steel structure (for which $k_0 - 50W/m/\text{deg.}$, say). It is easily inferred from (4) that λ would therefore generally exceed 1 m., and from (3) we note that we are implying heat transfer rates of up to $50kW/\text{sq.m.}$ Thus with material thicknesses of the order (say) of up to 1 cm. thickness, the value of (t_0 / λ) is less than 0.01. Further, the length ℓ would be calculated to be around 10 cm., and the temperature over this length of surface from the leading edge of a wing is a matter of some consequence.

If we introduce the non-dimensional notation

$$x/\ell = \xi, \quad T/T_0 = \theta, \quad kt/k_0 t_0 = K, \quad \varepsilon/\varepsilon_0 = e, \quad Q/Q_0 = q \qquad \ldots (5)$$

then the equation for heat conduction becomes

$$\frac{d}{d\xi} \left(K \frac{d\theta}{d\xi} \right) = e\theta^4 - q \qquad \ldots (6)$$

where $\theta \equiv \theta(\xi)$, and K, e, q may be generally functions of ξ and possibly θ. It is not difficult to generalise to 3 dimensions by introducing a third co-ordinate $y = \eta \ell$, say, and we then have $\theta \equiv \theta(\xi, \eta)$ where

$$\frac{\partial}{\partial \xi} \left(K \frac{\partial\theta}{\partial \xi} \right) + \frac{\partial}{\partial \eta} \left(K \frac{\partial\theta}{\partial \eta} \right) = e\theta^4 - q \qquad \ldots (7)$$

but the present discussion will be limited to examples of the two-dimensional solution.

Aside from the implication that θ, K, e and q are of unit order provided that the scaling terms are chosen in the manner we have suggested, we have not fully defined the notation in (5). Since, from (2) we have

$$\ell = (k_0 t_0 T_0 / Q_0)^{\frac{1}{2}} \qquad \ldots (8)$$

it will be seen that equations (8) and (3) together provide only two relations between the five disposable quantities ε_0, T_0, Q_0, $k_0 t_0$ and ℓ

which/

which enter into the definitions of (5). This leaves three further
relations to be invoked to specify the notation uniquely. It seems best
to leave this ambiguity unresolved for the moment.

2.1 Boundary Conditions

The solution of the equation (6) depends, of course, upon the
boundary conditions imposed, and these in turn depend upon the physical problem.
Generally, because the length ℓ may well be substantially less than that
length of surface subjected to heating, and because it is only over lengths
of this order that longitudinal conduction is important, it is convenient
to regard the conducting plate as of bounded extent, and insulated at the rear
edge (x = L) from the rest of the surface, which may be treated effectively
as non-conducting. Again, in experimental work, it is usually easiest to
terminate the extent of the body tested by insulation. Such considerations
lead us to expect that appropriate boundary conditions may frequently take the
form:

$$K \, d\theta/d\xi = 0 \quad \text{at} \quad \xi = 0 \quad \text{and} \quad \xi = L/\ell \qquad \dots \ (9)$$

This may be clearly acceptable if we suppose not merely that the
material thickness (t) vanishes outside the interval $0 < x < \ell$, but that
it tends to zero in some continuous manner as $x \to 0$ and $x \to L$, so that
$K \to 0$ continuously as $\xi \to 0$ and $\xi \to L/\ell$, since we could reject a finite
longitudinal heat flux through a vanishing cross sectional area as physically
unreal. As we shall now see, it is more difficult to justify in some
contexts, if t (and so K) is not zero at the limits of the range of
independent variable (though zero, or effectively so, outside them).

First let us then suppose that $K \, d\theta/d\xi = h$, where h is non-zero;
this implies that the longitudinal heat flux is $hQ_o\ell$. Then (9) might be
justified if we could show that the longitudinal heat flux to the ends of the
body (across the planes x = 0 and x = L) is small compared with the total
normal heat transfer over the length ℓ - since this ratio is of order h.
Now if the plane x = 0 represents the nose of a wing with thickness t_n, say,
then a study of aerodynamic heat transfer from a laminar boundary layer would
suggest that this ratio was of order $(t_n/\ell)^{\frac{1}{2}}$, and so from (2) of order
$(t_n/t_o)^{\frac{1}{2}}(t_o/\lambda)^{\frac{1}{4}}$. Thus the neglect of h at $\xi = 0$ is compatible with the
basic assumption that $(t_o/\lambda) \to 0$ though clearly in this context the
approximation is cruder (if $t_n \neq 0$) than that involved by the neglect of the
temperature difference across the surface. A similar argument can be used
to justify the neglect of h at the "downstream" limit $\xi = L/\ell$. In
application to the problem of aerodynamic heat transfer, this latter boundary
plane might be the trailing edge (where the local heat transfer is certainly
less than that at the leading edge), or some position where the thickness
changes discontinuously to a very small (effectively zero) value. In the
latter context, the downstream edge may be exposed to an interior cavity of
the structure, and again the heat flux to that edge may reasonably be taken as
less than that to an exposed leading edge. Thus the condition (9) is
relevant at least in an approximate sense to a wide range of problems.

As/

As a consequence of equation (9), we note that, for $\xi \to 0$

$$\theta \sim \theta(0) - \int_0^{\xi} (1/K) \left(\int_0^{\xi} q\,d\xi \right) d\xi + \mathcal{O}(\xi^2)$$

Thus, since the nose temperature must be bounded, we must find that

$$(\xi/K) \int_0^{\xi} q\,d\xi \to 0$$

as $\xi \to 0$. Where K_1 is $\mathcal{O}(\xi)$ so that the nose is sharp, we would generally expect that $q = \mathcal{O}(\xi^{-\frac{1}{2}})$ if the heating is aerodynamic in origin, unless the nose temperature were the thermometer temperature. Thus the latter condition will apply if, and only if, $K = \mathcal{O}(\xi^{3/2})$ for $\xi \to 0$. However, the cusped leading edge thereby implied is not thought to be of practical interest, and in fact we shall usually consider nose shapes which are rounded, or blunted. On the other hand a cusped rear edge (at $x = L$) will be found to lead to a temperature at this edge locally equal to the radiation equilibrium temperature, and this is clearly an acceptable possibility. Indeed, we shall have it in mind that the application of the work is to thin-skinned structures which may be locally thickened over a length L (of the same magnitude as the length ℓ) to enhance the effects of longitudinal conduction, and this extra material would be likely to be tapered off towards the rear.

2.2 Equations for plates of finite length

If the body has such a "closed" length (L), it is clearly possible, and in some instances preferable, to seek a solution of (6) in terms of the independent variable (x/L), rather than (x/ℓ); more particularly if we write

$$x/L = s, \quad kt = (\varepsilon_0 \sigma Q_0^3)^{\frac{1}{4}} L^2 \tau, \quad (\text{i.e.,} \ \tau = (\ell/L)^2 K) \qquad \ldots \ (10)$$

with θ, e and q defined as before, but regarded as functions of s, then equation (6) becomes

$$\frac{d}{ds}\left(\tau \, \frac{d\theta}{ds} \right) = e\theta^4 - q \qquad \ldots \ (11)$$

and this is solved subject to the boundary conditions that

$$\tau d\theta/ds = 0 \quad \text{at} \quad s = 0, 1 \qquad \ldots \ (12)$$

Note that $(k_0 t_0)$ does not need any longer to be defined in the notation of (10), as L has supplanted ℓ as a reference length. Nonetheless one must not allow this to cloud the fact that the solution is still valid only for $(t_0/\lambda) \to 0$, and in the notation of (10) for finite values of $(L/\ell)^2 \tau$

Trivial solutions result from (11) in two extreme cases. Thus if we allow $\tau(s) \to 0$, then $\theta \sim (q/e)^{\frac{1}{4}}$, or in other words the temperature tends everywhere to the radiation equilibrium value. On the other hand, if we suppose $\tau(s) \to \infty$, which can clearly only be justified where $(L/\ell) \to 0$ then

$$\theta(s) \rightarrow \left[\int_0^1 q\,ds \Big/ \int_0^1 e\,ds \right]^{\frac{1}{4}}$$

which is the solution for the condition of "infinite conductivity" in which the temperature is constant throughout; in particular, if we supposed that Q_0 and ε_0 represented the appropriate mean values $\bar{Q}$ and $\bar{\varepsilon}$ of Q and ε, then in this condition $\theta = 1$.

Note that, irrespective of the magnitude of r, it follows from (12) in (11) that

$$\int_0^1 e\theta^4\,ds = \int_0^1 q\,ds \qquad \qquad \dots (13)$$

that is, the total radiation emitted must balance the total heat flux to the body since the edges are supposed insulated, and consequently if the emissivity is constant (so that $e = 1$), the maximum value of θ is always in excess of the "infinite conductivity" value.

2.3 Factors affecting the method of solution

Even accepting the simplified equations, such as (6) and (11), as a basis for calculation of the temperature distribution, the implementation of a solution may still be difficult. These difficulties arise from two causes. First of all, the body may be non-homogeneous. Variations of material may be accommodated by interpreting the local value of kt as an integral of k across the thickness, but the presence of an internal cavity would properly require the condition of radiation equilibrium of the interior surfaces to be evaluated, and this involves the solution of an integro - differential equation. However, this difficulty is resolved if as here we are considering bodies which are geometrically thin, since in this limit, the condition of radiation equilibrium is satisfied by ignoring the change of temperature across the cavity. Thus, compatibly, the cavity is replaced by an insulator.

The second difficulty concerns the evaluation of the heat flux to the body surface. We have in mind the application where this is dominantly the heat transmitted from a boundary layer, and granting the likelihood that the boundary layer flow may be laminar, it might be possible to invoke theoretical values for this heat flux, if the surface temperature were known. Since it is not known, a priori, we would be faced with the need to adopt numerically some iterative approach, and this again is a considerable complication. However, where the thermometer temperature is large compared with the variation of surface temperature, - and certainly this would be the realistic condition in heat transfer to a body in flight at hypersonic speeds - it would be a reasonable approximation to ignore the dependence of q on θ, provided perhaps that the value of Q_0 included some dependence on (say) T_0. Then the remaining complication would arise from the influence of the shape of the exterior surface and the conditions of flight. If the exterior were wedge shaped then, setting aside boundary-layer shock-wave interaction, Q might be expected to vary as $1/x^{\frac{1}{2}}$. In practice, a sharp nose is undesirable, since it leads to an unduly high nose temperature and aggravates the problem of thermal buckling: nonetheless having recourse once again to the assumption

that/

that we are dealing with a body which may be geometrically thin, deviations from this form of variation of Q with x are likely to be small, even in application to blunt nosed wing sections.

2.4 Similarity relations

Let us suppose that some convention is to be consistently adopted by which the quantities ε_o, T_o, Q_o and $k_o t_o$, appearing in the notation of (5) and (10), are stipulated. Let us assume, for instance, that we place

$$Q_o = Q(L), \quad \varepsilon_o = \varepsilon(L), \quad \int_0^L ktdx = k_o t_o L \qquad \dots (14)$$

so that $q(1) = e(1) = 1$, T_o is from (3) the radiation equilibrium temperature at the rear edge, and

$$\int_0^1 r(s)ds = (\ell/L)^2 = (T_R/T_o)^3 = r_o, \quad \text{say} \qquad \dots (15)$$

where $T_R = (k_o t_o/\varepsilon_o \sigma L^2)^{1/3}$ is a "reference temperature" independent of the magnitude of heat input. Then for any problem in which, subject to the normalisation we have adopted, the functions $K = r/r_o$, q and e remain the same - that is, the thickness distribution, heat input and surface emissivity remain similar - a solution of (6) or (11) will result in which $\theta = T(x)/T_o$ will be a function of $s = x/L$ and of a parameter such as r_o, or (T_o/T_R), or (L/ℓ). At a fixed value of s (say $s = 0$, corresponding to the nose) the temperature will be a function only of this parameter.

One of the most convenient forms of these many possible variants of the expression for temperature in laboratory studies, where the level of heat input is easily adjustable (but the geometry remains fixed), is obtained by placing

$$T = T_R f(x/L, \ T_o/T_R) \qquad \dots (16)$$

where evidently $f \equiv (T_o/T_R) \ \theta$. Theoretically, the form of the relation f could be determined directly from a solution of the equations (11) and (12) with r, θ and q replaced respectively by $K = (r/r_o)$, f and $(Q/\varepsilon_o \sigma T_R^4)$. Equation (16) expresses the fact that to simulate in the laboratory a condition in which $T_o)$ is large, it is possible to work with much smaller levels of heat input (and so of T_o) provided that T_R is reduced in the same proportion, say by increasing L, or reducing $k_o t_o$.

Where the variation of Q as a function of x or s follows a simple power law, it is possible to assert similarity relations of still greater generality, and it is this which renders the assumption that Q varies as $x^{-\frac{1}{2}}$ of particular interest, whatever the misgivings one may feel about the accuracy of the assumption.

2.5 Solution for Q varying as $x^{-\frac{1}{2}}$

We shall here place $Q = Hx^{-\frac{1}{2}}$, and we shall assume for simplicity that $\varepsilon = \varepsilon_0$ and $k = k_0$ are constants. We adopt the conventions of (14), whereby we set $Q_0 = HL^{-\frac{1}{2}}$ and choose t_0 as a mean thickness in the sense that $t_0 = A/L$ where A is the cross-sectional area of the thickness distribution. It does not of course matter whether we choose (6) or (11) as the equation to be solved: we shall prefer to treat the latter, and in terms of the notation just introduced, we have

$$\theta = (T/T_0) = (\varepsilon_0^2 \sigma^2 L/H^2)^{1/8} T, \quad \tau = k_0 t/(\varepsilon^2 \sigma^2 H^6 L^{13})^{1/8}, \quad \tau_0 = k_0 A/(\varepsilon_0^2 \sigma^2 H^6 L^{21})^{1/8}$$

$$\dots (17)$$

and further $e = 1$ and $q = s^{-\frac{1}{2}}$. The solution for $\theta \equiv \theta(s)$, say, will evidently depend not only upon the form of variation of the thickness distribution $K(s) = (\tau/\tau_0)$, but also upon the parameter τ_0, which is given in (17) in terms of its definition in (15), and which we shall prefer to use here rather than other parameters such as (L/ℓ) or (T_0/T_R) - plainly this is once again merely a matter of choice. Consequently, we can represent the solution for a fixed variation $K(s)$ - that is, for a family of geometrically similar thickness distributions - in a number of different ways, as

$$T = (T_0 \tau_0^{-m}) \theta(s) \tau_0^m$$

where m is of course arbitrary. However, if we suppose that one of the geometrical parameters (say, A) is to be regarded as a constant while we imagine another to vary (say, L), then it is convenient to choose the value of m so that $(T_0 \tau_0^{-m})$ depends on the fixed parameters; the effect of the variable geometry is then immediately shown by the variation of $\theta(s)\tau_0^m$ with τ_0. Since we shall have frequent recourse to this artifice, it is convenient to summarise these relations, as follows:

$$T = (H^2/\varepsilon_0^2 \sigma^2 L)^{1/8} \theta(s) \qquad \text{(length fixed)} \qquad \dots (18.1)$$

$$= (H^6/\varepsilon_0^5 \sigma^5 k_0 A)^{1/21} \theta(s) \tau_0^{1/21} \qquad \begin{array}{c}\text{(cross-sectional area} \\ \text{fixed)}\end{array} \qquad \dots (18.2)$$

$$= (H^4/\varepsilon_0^3 \sigma^3 k_0 t_0)^{1/13} \theta(s) \tau_0^{1/13} \qquad \text{(thickness fixed)} \qquad \dots (18.3)$$

$$= [H^3/\varepsilon_0^2 \sigma^2 k_0 (t_0/L^{1/2})]^{1/9} \theta(s) \tau_0^{1/9} \qquad \text{(nose radius fixed)} \qquad \dots (18.4)$$

$$= (H^2 L/\varepsilon_0 \sigma k_0 t_0)^{1/5} \theta(s) \tau_0^{1/5} \qquad \text{(fineness ratio fixed)} \qquad \dots (18.5)$$

$$= (k_0 t_0/\varepsilon_0 \sigma L^3)^{1/3} \theta(s) \tau_0^{-1/3} \qquad \text{(geometry fixed)} \qquad \dots (18.6)$$

The last of these relations is identical with (16) and is included here only for the purposes of consistency: it is of use where the geometry (i.e., t_0 __and__ L) may be known, and H is treated as variable.

Equation (11) has been solved for three examples of simple variations of $K(s)$, corresponding to 1 (a uniform thickness distribution), $3s^{\frac{1}{2}}/2$ (a parabolic distribution) and $2s$ (a wedge), by using the Runge Kutta process, with the help of a digital computer.

If we consider a plate of constant thickness, then $K = 1$ or $\tau = \tau_0$ and the values of nose temperature are shown in fig.1 plotted against τ_0. If the surface length is fixed, $\theta(o)$ tends to a finite limit as $\tau_0 \to \infty$ i.e., as $k_0 t_0$ is increased, corresponding in the limit to the "infinite conductivity" solution. In fact, as $\tau_0 \to \infty$

$$\theta(o) \sim 2^{1/4} + (1/5\tau_0) + \mathcal{O}(\tau_0^{-2})$$

On the other hand, as $\tau_0 \to 0$, then for a fixed $k_0 t_0$, the length L of the surface increases and T tends to a finite limit: that is, in (18.3), $\tau_0^{1/13}\theta(o)$ must remain finite in the limit, and we find in fact that

$$\theta(o) \sim 1.3058\tau_0^{-1/13} \quad \text{as} \quad \tau_0 \to 0$$

This merely tells us that indefinite extension of the material downstream has ultimately no effect upon the nose temperature. Indeed for a length of surface defined by a value of $\tau_0 = 1$, the nose temperature (with fixed $k_0 t_0$) is within 1% of the limit for an indefinitely long plate, and from (15) this clearly corresponds with the choice of the length L as identical with ℓ.

It will be seen that $\theta(o)\tau_0^{1/21} \to \infty$ in either limit $\tau_0 \to 0$ or $\tau_0 \to \infty$, and from (18.2) it follows that there will be some value of τ_0 for which the nose temperature is a minimum if A is fixed: this may be termed an optimum selection of τ_0, since it implies a "best use" of a fixed quantity of material. It appears that $\theta(o)\tau_0^{1/21}$ has a minimum value of 1.309 at about $\tau_0 = 2.0$ (the precise value being very ill defined, as the temperature is within 1% of the minimum for all values of τ_0 between 0.8 and 5). Thus from (17) and (18.2), for this optimum surface

$$L = 0.77(k_0^4 A^4/\varepsilon_0 \sigma H^9)^{2/21}, \quad t_0 = 1.30(\varepsilon_0^2 \sigma^{-3} H^6 A^{13}/k_0^8)^{1/21}$$
$$\text{for which} \quad T(o) = 1.309(H^6/\varepsilon_0^5 \sigma^5 k_0 A)^{1/21} \qquad \qquad \text{... (19)}$$

The temperature at the rear of the conducting slab varies from a value given by $\theta(1) = 1$ if $\tau_0 = 0$ (corresponding to the radiation equilibrium temperature if $k_0 t_0 = 0$), up to a value of $\theta(1) = 2^{\frac{1}{4}}$ if $\tau_0 = \infty$ corresponding to the "infinite conductivity" solution; this variation is shown in figure 2. Note that for $\tau_0 = 1$, although the nose temperature is within 1% of the value for an infinitely long surface of the same thickness, the temperature at the rear is over 10% above the radiation equilibrium value. Fig.3 is a sketch of some typical temperature distributions, in which θ is plotted versus ξ.

Similar sets of graphs in figs.4 - 6 and figs.7 - 9 relate respectively to the general family of parabolic and wedge distributions of thickness (i.e., with $K(s) = 3s^{1/2}/2$ and $2s$ respectively). In both cases, $\tau_0 \to \infty$ relates to the "infinite conductivity" solution, but as $\tau_0 \to 0$, we note that

$$\theta(o) \sim 1.688\tau_0^{-1/5} \qquad \text{for the wedge}$$

$$\theta(o) \sim 1.376\tau_0^{-1/4} \qquad \text{for the parabola}$$

the first relation showing (from equation (18.5)) that for a fixed wedge angle, indefinite extension of the material downstream has no effect, and the latter

relation/

relation showing the same thing for a fixed nose radius of curvature of the parabola from equation (18.4), since the nose radius of a parabola is $(9t_0{}^2/32L)$. For the wedge, the minimum nose temperature for a fixed area of material is given by setting

$$L = 0.38(k_0{}^4 A^4/\varepsilon_0 \sigma H^3)^{2/21}, \quad t_0/L = 6.9(\varepsilon_0{}^4\sigma^4 H^{12}A^5/k_0{}^{16})^{1/21}$$
$$\left.\begin{array}{l} \\ \text{for which} \quad T(o) = 1.4127(H^6/\varepsilon_0{}^5\sigma^5\ k_0 A)^{1/21} \end{array}\right\} \quad \ldots (20)$$

where (t_0/L) is the tangent of the wedge-semi-angle; for the parabola the optimum use of material is obtained with

$$L = 0.59(k_0{}^4 A^4/\varepsilon_0 \sigma H^3)^{2/21}, \quad r_n = 9t_0{}^2/32L = 3.6(\varepsilon_0 \sigma H^3 A^3/k_0{}^4)^{2/7}$$
$$\left.\begin{array}{l} \\ \text{for which} \quad T(o) = 1.3428(H^6/\varepsilon_0{}^5\sigma^5 k_0 A)^{1/21} \end{array}\right\} \quad \ldots (21)$$

Comparing equations (19) to (21) we see that the uniform plate makes the best use of the material, and the wedge the poorest use, reflecting the special importance of material near the leading edge in alleviating its temperature.

It is pertinent to enquire what variation of $r(s)$ has to be assumed in order to render $T(o)$ a minimum if the cross section area A of the thickness distribution is prescribed. This precipitates an exercise in the calculus of variations which is algebraically rather involved, and will not be detailed here. It transpires that the shape has no closed algebraic description, but can be derived by numerical calculation. It has a blunt nose, with r varying locally as $s^{1/4}$ so that the nose radius is infinite; and a cusped rear edge, with r varying locally as $(1 - s)^{1/2}$. The maximum thickness occurs at 0.07L, and is equal to 2.48 t_0, where t_0 as in (14), is the mean thickness. There is an optimum selection of length, associated of course with an optimum fineness ratio, and this leads to a unique optimal variation of r with s, which is given in table I. The corresponding value of r_0 is equal to 0.6983; the temperature distribution is shown in fig.10, and the value of $\theta(o)$ is found to be 1.309, so that we may find from (17) and (18.2) that

$$L = 1.143(k_0{}^4 A^4/\varepsilon_0 \sigma H^3)^{2/21}, \quad t_0 = 0.885(\varepsilon_0{}^2\sigma^2 H^6 A^{13}/k_0{}^8)^{1/21}$$
$$\left.\begin{array}{l} \\ \text{for which} \quad T(o) = 1.286(H^6/\varepsilon_0{}^5\sigma^5 k_0 A)^{1/21} \end{array}\right\} \quad \ldots (22)$$

There is a modest (2%) decrease in nose temperature compared with the optimum uniform slab but note that this implies that, to achieve the identical nose temperature, the slab would need to have 45% more cross-sectional area. Figure 11 extends this comparison to the other shapes discussed, by illustrating the optimum thickness distribution on common scales of length and thickness; the actual length and thickness scales, and their relative proportions in this illustration, would depend of course not only on the value of A, but also on conductivity, emissivity and the value of H; consequently the fineness ratios illustrated in fig.11 are not necessarily optimal.

Also included in this illustration is one of a family of distributions which provide a uniform temperature gradient. The evaluation of a thickness distribution for a given variation of θ is an easier problem, as then of course (6) or (11) become directly integrable equations for K or r, and in particular from (11),

$$r/$$

$$\tau(s) = [1/\theta'(s)] \left[\int_0^S (e\theta^4 - q)\, ds \right] \qquad \ldots (23)$$

where $\theta'(s) \equiv d\theta/ds$. The mean value of θ cannot be allowed to be arbitrary if Q_0 and ε_0 are stipulated, since equation (13) has to be satisfied, and this simply means that since the temperature determines the total heat radiated, it has necessarily to be related to the total heat input to the surface. Furthermore, the fact that τ must be bounded and cannot be negative imposes restraints on what temperature distributions can be realistically postulated. Thus if, for example, we postulate, using the notation of equation (23) and (15), a temperature distribution given by

$$\theta(s) = \theta(o)\ (1 - \alpha s)$$

then from (13), since $e = 1$ and $q = s^{-\frac{1}{2}}$

$$\theta(o) = \{ 10\alpha / [1 - (1 - \alpha)^5] \}^{\frac{1}{4}} \qquad \ldots (24)$$

and (23) leads to a thickness distribution given by

$$\tau(s) = [2/\alpha\theta(o)]\ \{ s^{\frac{1}{2}} - [1 - (1 - \alpha s)^5]/[1 - (1 - \alpha)^5] \}$$

This has real solutions (corresponding to bounded $\tau \geqslant 0$ for all $0 \leqslant s \leqslant 1$) $0 < \alpha \leqslant 0.26057$. The lower limit of vanishing temperature gradient ($\alpha \to 0$) corresponds, as might be expected, to the "infinite conductivity" solution, for which $\theta(o) \to 2^{\frac{1}{4}}$, and

$$\tau(s) \sim (s^{\frac{1}{2}} - s)/\alpha$$

as $\alpha \to 0$. This is of course only valid in the limit if $L/\ell = O(\alpha^{\frac{1}{2}})$. The other extreme condition ($\alpha = 0.26057 \ldots$) is more interesting. The thickness distribution associated with it is characterised by a cusped trailing edge, with τ varying locally as $(1 - s)^2$, and the local temperature is precisely the radiation equilibrium value (i.e., $\theta(1) = 1$): in fact this value of α is found by solving the equation obtained by replacing $\theta(o)$ in (24) with $1/(1 - \alpha)$. The shape has a rounded nose, and a maximum thickness 2.34 times the mean, located at a distance $0.114L$ from the nose. The value of $\theta(o)$ is 1.353, and $\tau_0 = 0.379$. Of all the members of this family of thickness distributions providing uniform temperature gradient, which are generated by varying α (and are not of course geometrically similar), it provides the least nose temperature for a given cross sectional area. We find in fact that

$$L = 1.45\ (k_0^4 A^4/\varepsilon_0\sigma H^3)^{2/21}, \quad t_0 = 0.69\ (\varepsilon_0^2\sigma^2 H^6 A^{13}/k_0^8)^{1/21} \left.\right\} \quad \ldots (25)$$

$$\text{for which} \quad T(o) = 1.289\ (H^6/\varepsilon_0^5\sigma^5 k_0 A)^{1/21}$$

Comparing (25) with (22) we see that this nose temperature is only 0.3% higher than that of the optimum shape, and it seems reasonable to suppose that the efficiency of both is in part due to the tapering off of the thickness distribution towards the rear, where of course there is less effect to be derived from the provision of conducting material.

To provide some feeling for what these numbers mean, let us suppose that $H = 10 kW/m^{3/2}$, which represents a heat input of 20 kW/m span over the first meter of the chord of a wing, and which might be taken as indicative of aerodynamic heating intensities in flight at hypersonic Mach numbers. Further let us take $\varepsilon_0 \sigma = 10^{-10}$ kW/m^2/(deg.K)^4 (corresponding to radiation from both upper and lower surfaces with emissivity 0.88), and $k_0 = 0.05$ kW/m/deg.K, a figure typical of steel. Table II evaluates the lengths, thickness and extreme temperatures of the various optimally selected surfaces, assuming in each case that a cross-sectional area of 10 cm^2 is available to be distributed (i.e. say 8 kg. of steel per meter span). Note, however, that even if this cross section is reduced to 1 cm^2, then provided the material is correctly redistributed - that is the length of surface is reduced by a factor $0.1^{8/21} = 0.42$, the thickness by $0.1^{13/21} = 0.24$ and so the fineness ratio increased by $10^{5/21} = 1.73$, - it follows from (18), or any of the relations in (19), (20), (21) or (25) that the nose temperature is increased by a factor of only $10^{1/21} = 1.116$. The same result applies if the conductivity is reduced to a tenth of its value for steel, provided the new material is suitably redistributed. Where such optimal redistribution is not affected, but (say) length, or conductivity, is changed in isolation, then larger variations in nose temperature will be manifest, and these cannot in general be predicted except by recourse to the figures for the variation of (say) $\theta(o)$ with τ_0. But the same power laws as quoted here will apply for small, isolated changes in any feature (such as A or k_0) away from the optimum value (since $\theta(o)\tau_0^{1/21}$ has a stationary value in the optimum condition). In the same way that the nose temperature is relatively insensitive to the amount of material, so also, for an optimal surface this temperature is not very sensitive to the heat transfer intensity, varying only as $H^{2/7}$ (that is, $T(o)$ increasing by only 22% if the heating is doubled).

2.6 Solution for Q varying as $(x + x_0)^{-\frac{1}{2}}$

In experimental applications, the singularity associated with a heat transfer distribution varying with $x^{-\frac{1}{2}}$ cannot of course be realised. In order to determine how important this is in determining the heat transfer distribution we place

$$Q = H/(x + x_0)^{\frac{1}{2}} = (H/L^{\frac{1}{2}})/(s + s_0)^{\frac{1}{2}}$$

and examine the effect of varying $s_0 = x_0/L$. Results for a particular example are shown in fig.12: here t_0, k_0 and ε_0 are supposed constant, and the value of τ_0, given in terms of H by equation (17), is equal to 5.36, - a value chosen as relevant to the experimental investigation discussed in the next paragraph.

3. Experimental Investigation

The purpose of the investigation is twofold. In the first place we seek experimental verification of the leading edge temperature distribution predicted by the conducting plate theory given in section 2. Within the context of the theory, the model which represents the leading edge is subjected to a heat flux distribution varying roughly in proportion to $1/x^{\frac{1}{2}}$ along the length on one surface, and is insulated thermally on all other surfaces. The experimental apparatus so set-up may also provide some analogous studies of two-dimensional problems whose numerical solution may be specially difficult.

3.1 Simulation of aerodynamic heating

A number of methods could be adopted to simulate aerodynamic heating in the laboratory, but the simplest approach by far is to use infra-red radiation derived from electric power, provided that the intensity of the radiation distribution can be made to represent the convective heat transfer of the boundary layer. Our concern, therefore, is to simulate on a given plane a radiation field with an intensity varying as closely as possible with x^{-2}, so that when a model is placed with one surface lying in this plane, its leading edge (at $x = 0$) will be subjected to the highest heating. This is accomplished by employing a reflector formed so that a large portion of the energy emitted from a single heating element is reflected to impinge (together with the direct radiation) on the irradiated plane with the desired distribution.

The necessary differential equations for the design of the reflector are given in references 4 and 5. Its actual size and shape are directly influenced by many parameters, such as the distance between the heating element and the irradiated plane, the size of the model, the size of the heating element as well as the location of the reflector relative to the element. Hence it is possible to have different shapes of reflectors resulting in the reflected rays crossing or not crossing each other. Radiation may also be reflected from different portions of the reflector to impinge on the same region on the irradiated plane, but those to impinge on the region of the leading edge must not be intercepted by the heating element itself after reflection. An acceptable solution can only be obtained with the help of digital computer calculations. Even then a number of practical difficulties remain. For example, to direct a large amount of radiation energy on to a very small region at the leading edge requires an extremely accurate profile of the reflector which must also possess a perfect reflecting surface. Any small deviations from perfect conditions will alter the direction of the incident rays and will cause them to diffuse. It follows that both the magnitude and the gradient of the radiation intensity will be substantially reduced, especially over the leading edge region, if any small imperfections are present. To alleviate these shortcomings, an arrangement is made, again with the help of a digital computer, for the profile of the reflection to be composed of a number of curves each of which is similarly designed to produce the desired distribution of radiation, with the highest intensity always directed towards the nose. Altogether there are seven curved surfaces blending smoothly to form a quasi-continuous profile.

In construction, the reflector was fabricated by a sheet of highly polished copper over a solid block made to conform first of all to the prescribed profile. Once the sheet was firmly pulled over the block, the over-hanging parts of the sheet were attached to two end plates, made of aluminium alloy to the same profile. Thus the sheet could be held permanently to the required shape.

To avoid distortion of the reflector by heat during its operation, cooling of the black surface is provided by circulating cold water through bonded copper tubes. The end plates were coated with a black paint to give a high absorptivity and are also cooled during experiments.

The heat source is a wire coiled round a ceramic tube, which is reinforced by the insertion of a tungsten rod to prevent sagging at high temperatures, giving an overall diameter of the heating element of 0.57 cm.

Oxidized/

Oxidized nickel wire was first used because of its high emissivity at elevated temperatures. Operating in vacuo, however, this material tends to become unstable when operating temperature exceeds 1000°C. The maximum power output of the element over a length of 0.305 m (the length of the reflector) was 1.2 kW. In order to increase the power output, the nickel wire was subsequently replaced by a tantalum wire which, though having a much higher melting temperature, possesses only a moderate emissivity. To improve its emissive power, the tantalum wire was oxidized in air at a temperature of 550°C for 30 minutes. At higher temperatures, the material is liable to decompose owing to the rapid process of oxidation. Using the oxidized tantalum wire, the maximum heating power was increased to 1.8 kW.

The reflector was tested in a vacuum chamber and its performance was recorded by a radiometer specially designed for the purpose (ref.6). The results are shown in fig.15. As can be seen, the measured results fit the ideal distribution fairly well up to a distance of s = 0.0275 from the leading edge, within which region the intensity of radiation does not increase as rapidly as required by the $x^{-\frac{1}{2}}$ law. To place the leading edge of a test model at s = 0 would tend to moderate the temperature gradient in the nose region and this is clearly undesirable. Hence it was decided to place the nose of a test model at s = 0.0275 for in this way not only is the $x^{-\frac{1}{2}}$ distribution of radiation satisfied but also the experimental results thus obtained can be compared directly with the theoretical calculations of section 2.6. Thus in the notation of that paragraph, the experimental heat input corresponds to one with s_0 = 0.0275. Typically, fig.12 shows that this would cause a difference of about 5 per cent in nose temperature compared with the ideal distribution (with s_0 = 0).

3.2 Test models

To verify the theoretical results, a model in the form of a slab is the simplest to construct and its performance is as informative as that of models of any other shape. Its size is largely determined by the dimensions of the vacuum chamber in which it and the heating element and reflector are installed. Its chord length is chosen as 15.25 cm. (6 in.) and its span as twice this in order to reduce the end effects on the central plane of the model where temperature measurements are made and two-dimensional conditions are expected to prevail. Over the top surface it is desirable to achieve a high surface emissivity. Other faces of the model will be insulated.

So long as the passage of heat by conduction from the nose towards downstream is nowhere restricted, the nose thickness has a dominant effect upon the temperature distribution. To observe this, trapezoidal sections of different nose thicknesses have also been tested (fig.17).

If we are interested in maintaining a certain temperature distribution in a model under a given heat input, the thickness of the model should bear an inverse proportion to the conductivity k, as the thickness t and k occur together in the simplified heat conduction equation. On the other hand to display the effects of conductivity over a reasonable proportion of its chord in association with the amount of heating available during experiment, the product of k and t is fairly closely defined. With the limited heating capacity available, it transpires that materials of relatively low thermal conductivity are preferred as only they provide a thickness sufficiently large to enable an easy observation of the temperature variation along the model. Figure 16 shows the variation of nose and rear temperatures with t for models of L = 15.24 cm (6 in.) having three different

fineness/

fineness ratios (i.e., L/t), taking $H = 1684 \, W/m^{3/2}$ and $\varepsilon = 0.8$.
(These preliminary results were obtained on the basis of $x^{-\frac{1}{2}}$ heat flux
distribution with $s_0 = 0$. The nose temperatures should have been 5% lower
had s_0 been taken as 0.0275). If high conducting materials such as
copper and aluminium were used, a near uniform temperature would result.
To produce a greater variation of temperature distribution, our choice should
fall on materials having a much lower k. Among common metals, stainless
steel F.C.B. Staybrite (AISI-347) with $k = 15.88 \, (1 + 3.898 \times 10^{-4} \, T^\circ C)$
$W/m^\circ K$ (7) appears to be a reasonable material to use. Ceramics have also
been considered. Generally, the low conductivity of this type of material
should satisfy the requirement very well but for the non-homogeneity in
properties and shrinkage liability during the firing process. However,
one type of ceramic known as Frequentite, bearing similar characteristics to
Steatite, and having a thermal conductivity $k = 3.17 \, (1 + 5 \times 10^{-4} \, T^\circ C)$
$W/m^\circ K$ is chosen.

Altogether ten models are used in the experiments. The details
are given in table III.

For the stainless steel models, the top surface was shot-blasted
and oxidised at a temperature of 900°C for 20 minutes. According to
reference (8), the emissivity is taken as $\varepsilon = 0.735 \, (1 + 2.944 \times 10^{-4} \, T^\circ C)$.
Other faces were highly polished to reduce the amount of heat loss to a
minimum.

For the ceramic model, the top surface was coated with lampblack
mixed with fibrefrax cement of which the emissivity is assumed to be 0.78.
Other faces were machined flat and then polished with diamond powders.

3.3 Apparatus

Aerodynamic heating to be simulated by infra-red radiation, and
heat dissipation from the model to be entirely due to radiation demand that
the presence of convective heat transfer be eliminated during experiment.
This requires both the reflector and the model to be housed in a vacuum
chamber. The model is supported by four pointed ceramic rods which in turn
rest on the side of four ceramic pins (fig.14), thus reducing any conduction
heat loss to a minimum. Apart from the top surface of the model which is
subjected to heating, the vertical as well as the bottom faces are shielded
against radiation heat loss. The walls of the vacuum chamber are painted
black, using Britannia D enamel paint, which is believed to have an
absorptivity of 0.9. During operation, the whole chamber is cooled by
circulating cold water through copper pipes welded round the chamber in
order to minimize background radiation. Temperature measurements, taken
along the middle section of the model at 6 prescribed locations, are by
means of nichrome - constantan (0.012 cm. diameter wires) thermocouples
which were calibrated by the National Physical Laboratory. Two rows of
thermocouples were placed at different depths in the model, one row near the
top surface and the other near the bottom surface to detect any variation of
temperature across the model thickness. The general lay-out of the
apparatus is shown in fig.13.

3.4 Experimental procedure and test results

To start the experiment, the vacuum chamber is evacuated by a
6" diffusion pump backed by a single-stage rotary pump. When the chamber

pressure reaches a value below 5 mN/m², electric current to heat up the element of the reflector is switched on. Both the current and the voltage drop are measured so that the total input power can be increased by definite increments. During each power increment temperature measurements by means of thermocouples using a potentiometer are taken as soon as the steady state condition is reached. The temperature distribution under maximum power input is used for comparison with the theoretical values. The test results are given in table IV.

To assess the amount of radiation impinging on the model, the radiometer mentioned earlier is used. But the amount of heat absorbed by the model can be taken to be equal to the amount of heat dissipated from the top surface of the model, on the assumption that any heat loss from elsewhere is negligibly small. Thus it can be calculated directly from the temperature distribution along the model. In table IV, the total power input to the heater is the direct reading from a wattmeter, while the power received by the model is accordingly the integration of the radiant heat dissipated from the model.

3.5 Comparison of theory with experiment

Fig.17 shows the calculated temperature distributions for the nine stainless steel models with $H = 7500$ W/m$^{3/2}$. They constitute a family of curves flanked by the radiation equilibrium temperature curve in one extreme and the infinite conductivity temperature in the other. By taking material conduction into account, the temperature at the nose and in the region near to it drops below the radiation equilibrium temperature, at the expense, apparently, of that at the rear. One important feature from the results given in fig.17 is worth mentioning. The reduction of nose temperature and of the temperature gradient along the whole length of the conducting plate can be significantly achieved by an increase in the nose thickness, which, we must accept, represents the quantity of conducting material employed at the most crucial position. Subjected to the same heating intensity, models of the same nose thickness, though having different shapes, give rise to more or less the same temperature distribution as shown by curves B, C and D. In fig.18, the calculated variations of nose and rear end temperatures are plotted against the heat flux parameter H using model 1 and model 6 in present experimental conditions.

Test results from the ten models are plotted in figures 19-28. The agreement between experiment and theory for models 1, 2, 3, 4, 5 and 7 are remarkably good. Considering that a number of errors, such as in temperature measurements, in the absolute quantities of k and ε and their variation with temperature and in the insulation of the model against heat loss, could have existed in the experiment, the maximum discrepency is only about 2%. This indicates that the temperature variation is not too sensitively influenced by any one parameter. The agreement between experiment and theory for the wedge models are not so good. In all three cases, the predicted temperatures are much higher than the calculated values at the nose. The maximum discrepancy is just over 5%. However, due to the machining and polishing processes, the thickness of a wedge nose cannot be clearly defined, and any small deviation in measurement from zero is known to have a disproportionate reduction upon the calculated values of nose temperature. Test results on the ceramic model follow the theoretical curve very closely, except that at the location adjacent to the nose.

The/

The temperature measured at this point is about the same as that at a point
1.27 cm. downstream. We consider this may have been due to the
malfunctioning of the thermocouple at this location. Under two different
inputs of heating, the temperature distribution in general behaves as
predicted.

The results obtained from two rows of thermocouples embedded at
different depths in the models indicate that there are negligible temperature
variations across the thickness.

4. Conclusions

The concept of a "conducting plate" simplifies the examination of
the role of longitudinal conduction of heat within the material of a wing
subjected to aerodynamic heat in hypersonic flight. Various similarity
laws result which provide a broad insight into the properties determining the
nose temperature. Moderate temperatures result from quite small provisions
of conducting material, and leading edge thicknesses of about 1 cm or so.
Experimental results closely verify the theory.

5. Acknowledgements

References/

Fig. 5. RATIO OF TEMPERATURE TO RADIATION EQUILIBRIUM TEMPERATURE AT REAR OF PARABOLIC BODY.

- 22 -
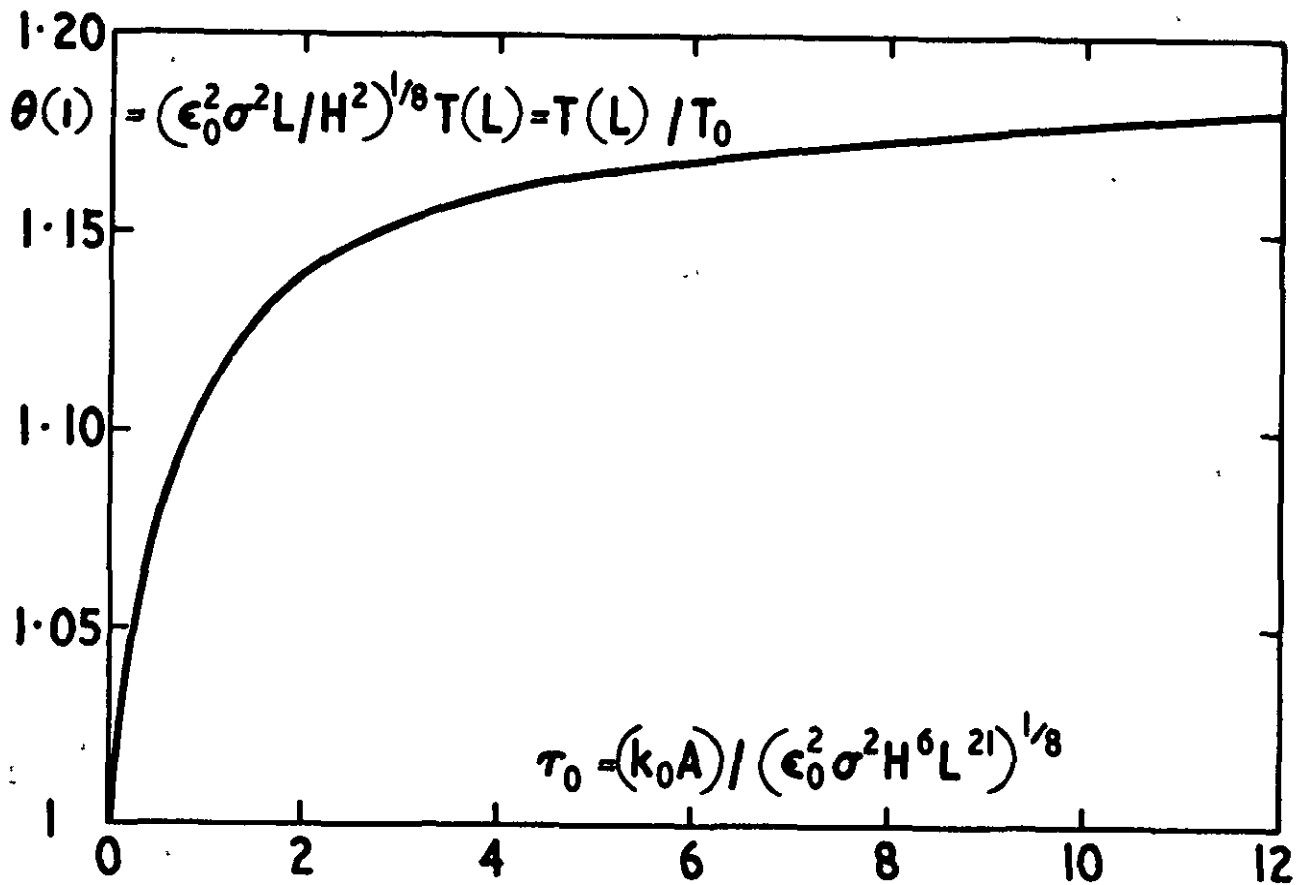
Table I

The optimum thickness distribution

$s^{\frac{1}{2}}$	$\tau(s)$	$s^{\frac{1}{2}}$	$\tau(s)$	$s^{\frac{1}{2}}$	$\tau(s)$
0	0	0.35	1.6558	0.70	0.5740
0.05	1.0142	0.40	1.5574	0.75	0.4138
0.10	1.3625	0.45	1.4277	0.80	0.2729
0.15	1.5681	0.50	1.2742	0.85	0.1571
0.20	1.6825	0.55	1.1047	0.90	0.0710
0.25	1.7273	0.60	0.9265	0.95	0.0181
0.30	1.7152	0.65	0.7472	1.00	0

Table II

Typical characteristics of optimised thickness distributions

Body Shape	Length (cm)	Mean thickness (cm)	Maximum thickness (cm)	Position (cm from nose)	Nose temp. (°K)	Rear-edge temp. (°K)	λ (m)	Remarks
Optimal distribution	12.1	0.83	2.05	0.85	956	732	1.2	
Uniform temperature gradient	15.4	0.65	1.52	1.76	959	789	1.4	Nose Radius = 7.5mm
Uniform Thickness	8.2	1.22	1.22	–	974	876	1.1	
Parabolic	6.3	1.59	2.38	6.3	999	920	1.0	Nose Radius = 2.5mm
Wedge	4.1	2.44	4.88	4.1	1051	989	0.85	Semi-apex angle = 30°

Table III

Test Models

Model No.	Material	Description
1	Stainless Steel (AlSl-347)	Slab $\quad$ a = b = 1.27 cm
2	"	Slab $\quad$ a = b = 0.635 cm
3	"	Slab $\quad$ a = b = 0.317 cm
4	"	Trapezoidal $\quad$ a = 0.635 cm $\quad$ b = 1.27 cm
5	"	Trapezoidal $\quad$ a = 0.317 cm $\quad$ b = 1.27 cm
6	"	Wedge $\quad$ a = 0.0508 cm $\quad$ b = 1.27 cm
7	"	Trapezoidal $\quad$ a = 0.317 cm $\quad$ b = 0.635 cm
8	"	Wedge $\quad$ a = 0.0254 cm $\quad$ b = 0.635 cm
9	"	Wedge $\quad$ a = 0.0254 cm $\quad$ b = 0.317 cm
10	Ceramic (Frequentite)	Slab $\quad$ a = b = 1.27 cm

Note: For all models, d = 30.48 cm, L = 15.24 cm.   See Figure 29.

Table IV

Experiment Results

Model No.	Total Power from heater (W)	Power received by model (W)	H $(W/m^{3/2})$	Temperature distribution °K					
				S=.0208	.1043	.271	.397	.647	.96
1	1806	237.5	1179	609.0 607.4	605.0 604.1	595.8 595.2	583.4 582.6	569.2 568.2	559.1 557.9
2	1748	213.5	1165	619.8 616.8	611.8 613.1	598.9 598.3	580.6 580.6	554.2 560.2	545.7 548.2
3	1889	258.2	1281	654.4 658.2	629.8 648.5	613.9 621.6	589.9 593.8	560.5 565.0	543.5 548.7
4	1852	246.0	1220	625.5 623.9	618.8 617.6	603.5 602.1	– 585.8	– 568.2	– 558.4
5	1835	236.0	1167	628.7 629.5	– 619.5	598.1 598.9	– 578.5	– 558.3	545.4 547.6
6	1886	240.6	1192	646.7 660.4	638.5 636.2	599.6 602.6	574.5 574.7	553.2 553.4	544.8 544.3
7	1866	255.2	1266	651.0 653.0	643.2 643.5	617.1 616.4	589.4 588.6	563.2 563.3	550.7 542.8
8	1886	247.7	1228	683.2 678.1	650.0 647.3	610.0 608.7	574.2 573.9	548.9 554.7	541.2 541.6
9	1868	240.2	1190	667.6 669.4	645.4 642.6	605.3 604.1	571.8 572.1	547.1 551.2	535.1 540.2
10	800	88.6	440	487.1 482.2	485.7 482.8	474.9 474.1	457.5 –	441.4 440.9	430 –
10	1200	127.1	631	537.7 528.5	535.6 531.1	520.9 519.2	501.2 –	479.9 479.2	465.8 –

Note: For each model the upper row temperatures were taken near the top surface while the lower row temperatures near the bottom surface.

$$\theta(0)\,\tau_0^{1/13} = (\epsilon_0^3 \sigma^3 k_0 t_0/H^4)^{1/13}\,T(0) \quad \text{THICKNESS FIXED}$$

CROSS-SECTIONAL AREA FIXED

$$\theta(0)\,\tau_0^{1/21} = (\epsilon_0^5 \sigma^5 k_0 A/H^6)^{1/21}\,T(0)$$

$$\theta(0) = (\epsilon_0^2 \sigma^2 L/H^2)^{1/8}\,T(0) \quad \text{LENGTH FIXED}$$

$$\sim 2^{1/4} + \frac{0.2}{\tau_0} \longrightarrow$$

$$\tau_0 = (k_0 A)/(\epsilon_0^2 \sigma^2 H^6 L^{21})^{1/8}$$
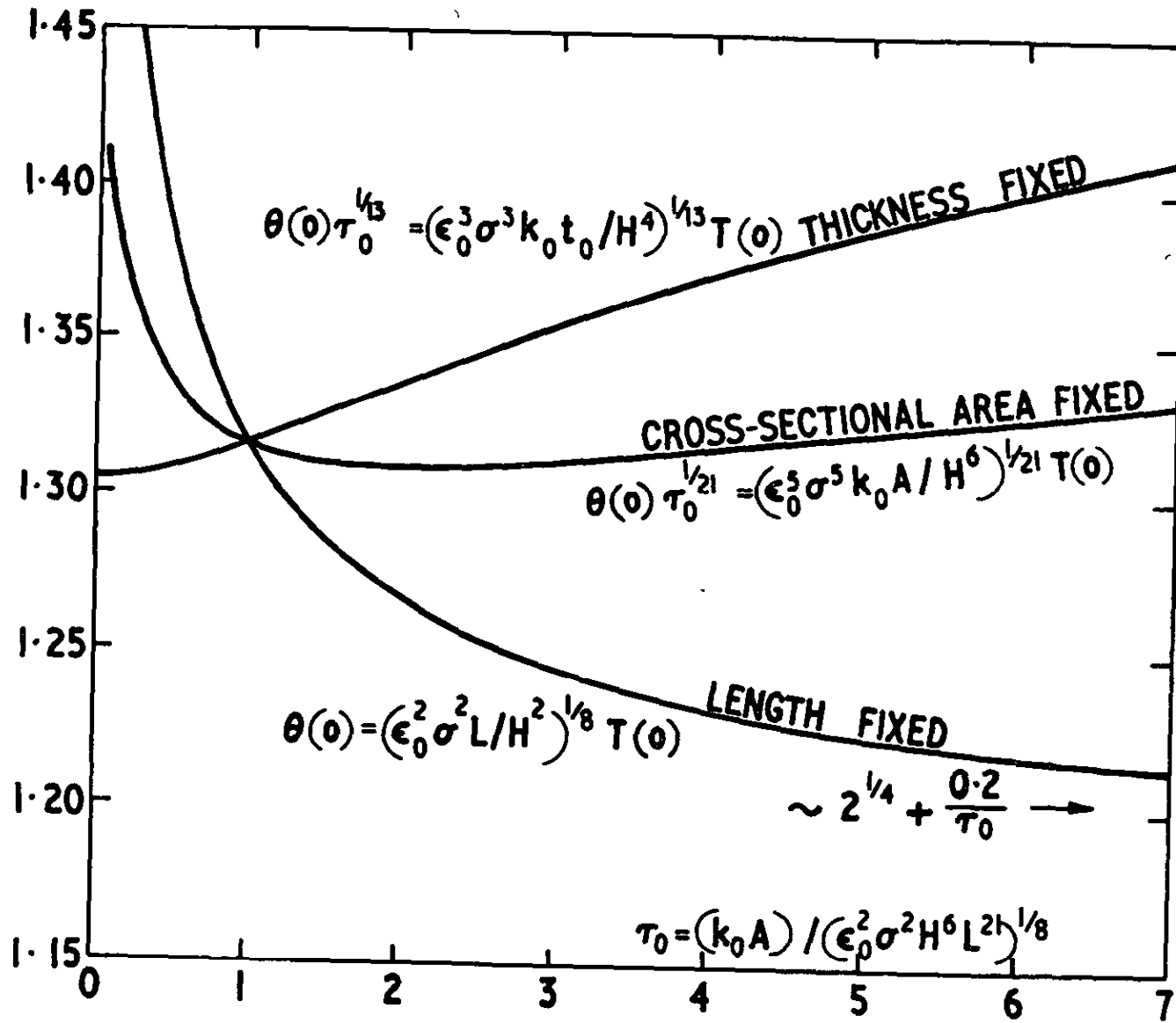
Fig. 1. NOSE TEMPERATURE FOR UNIFORM THICKNESS DISTRIBUTION $(t_0 = A/L)$

$$\theta(1) = \left(\epsilon_0^2 \sigma^2 L / H^2\right)^{1/8} T(L) = T(L)/T_0$$

$$\tau_0 = (k_0 A) / \left(\epsilon_0^2 \sigma^2 H^6 L^{21}\right)^{1/8}$$
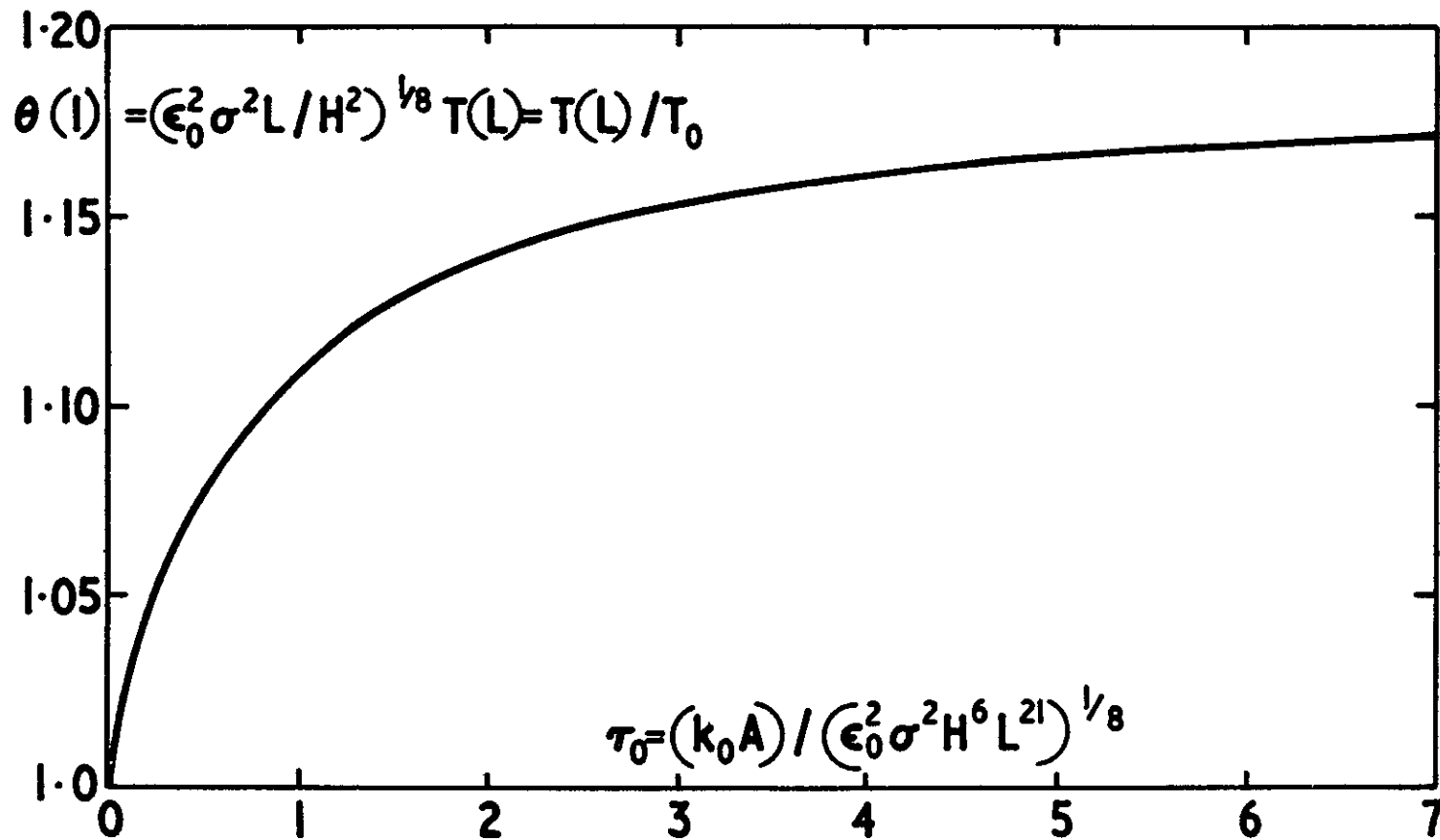
Fig. 2. RATIO OF TEMPERATURE TO RADIATION EQUILIBRIUM
TEMPERATURE AT REAR OF UNIFORM THICKNESS
DISTRIBUTION.

$$\theta \tau_0^{1/13} = \left(\epsilon_0^3 \sigma^3 k_0 t_0 / H^4 \right)^{1/13} T$$

REAR-EDGE
TEMPERATURE

RADIATION
EQUILIBRIUM
TEMPERATURE

$$\left(\epsilon_0 \sigma H^3 / k_0^4 t_0^4 \right)^{2/13} x$$
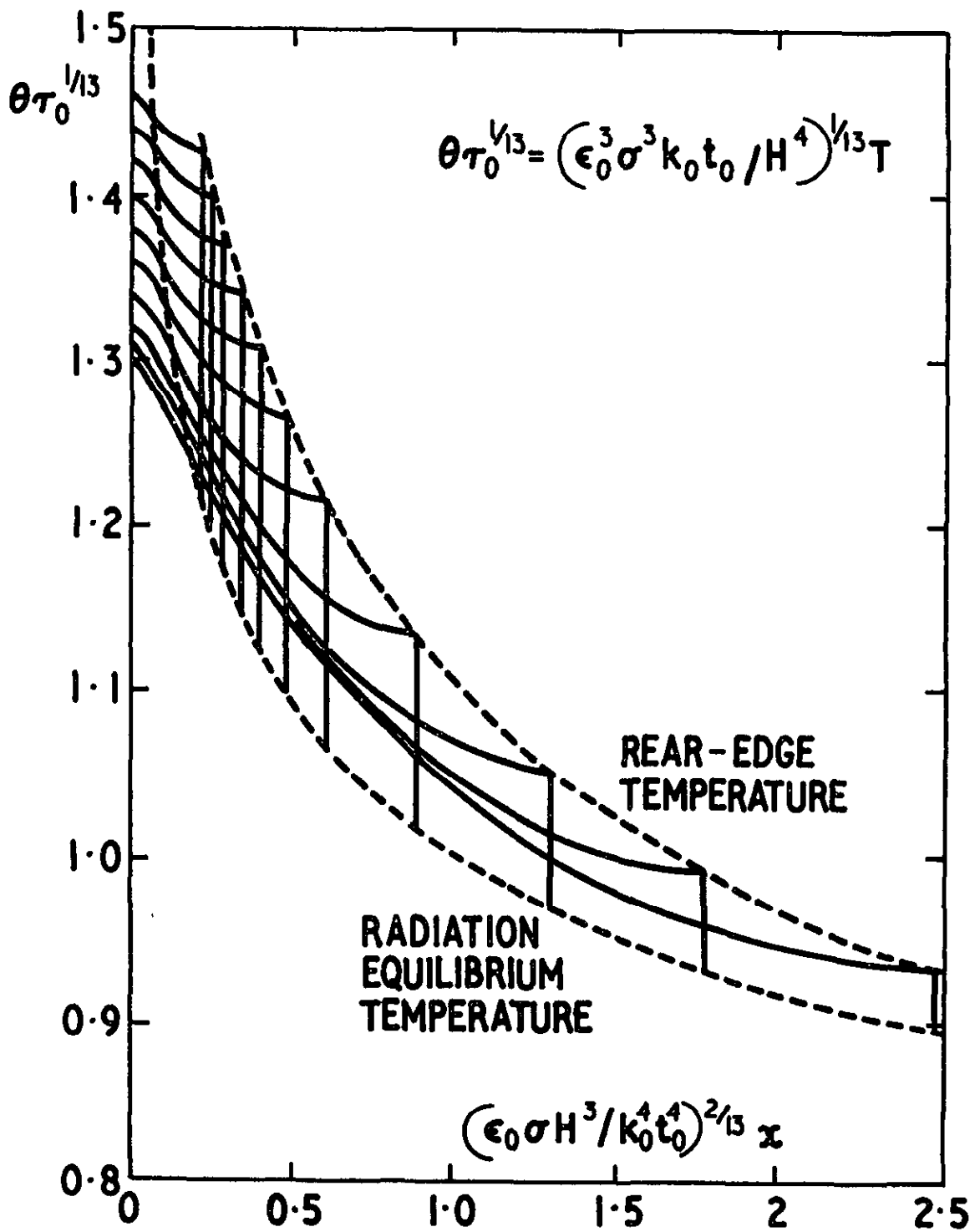
Fig. 3. SOME TEMPERATURE DISTRIBUTIONS
ALONG BODIES OF UNIFORM
THICKNESS.
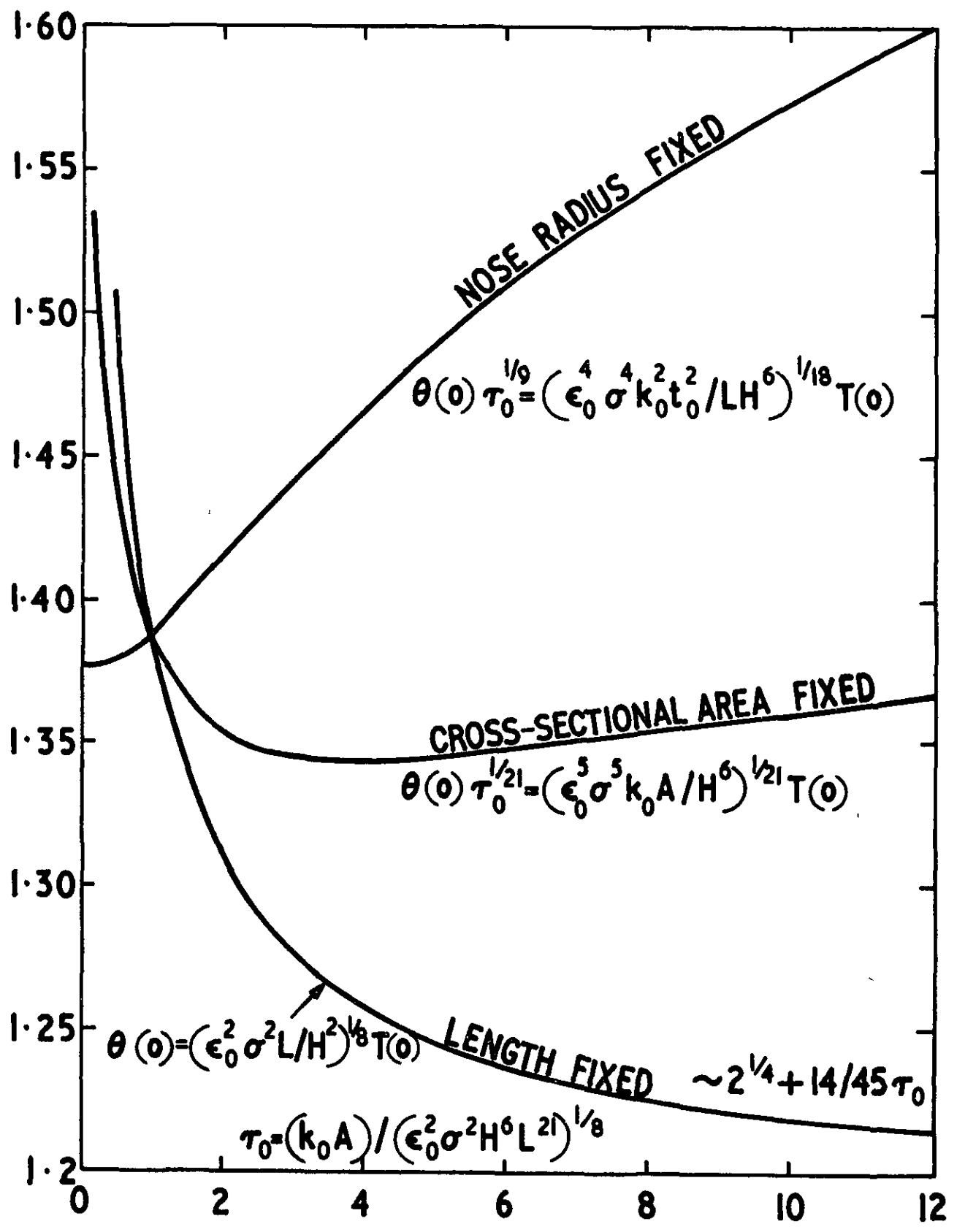
Fig. 4. NOSE TEMPERATURE FOR A PARABOLIC DISTRIBUTION OF THICKNESS (NOSE RADIUS = $9t_0^2/32L$)

Fig. 5. RATIO OF TEMPERATURE TO RADIATION EQUILIBRIUM TEMPERATURE AT REAR OF PARABOLIC BODY.
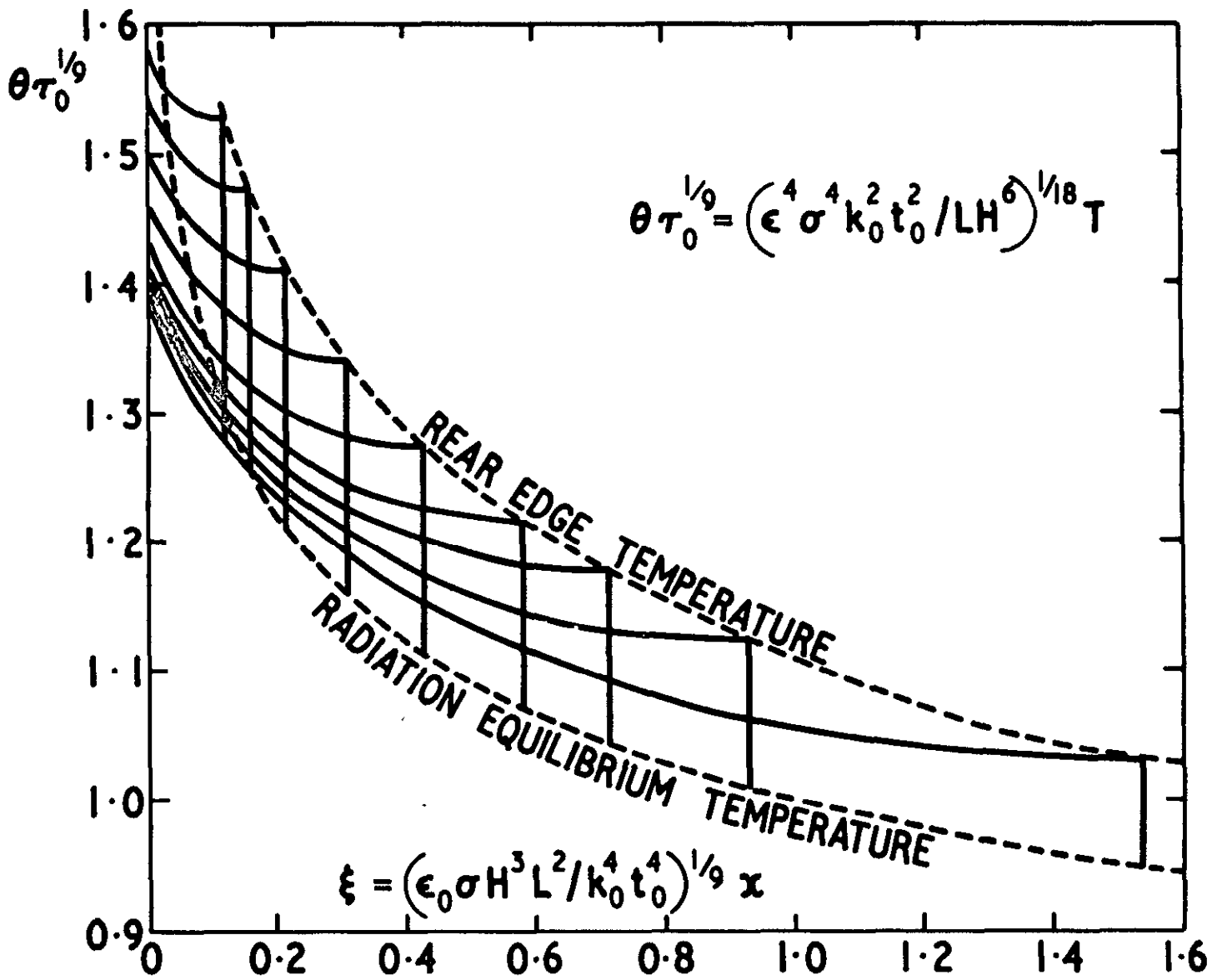
Fig. 6. SOME TEMPERATURE DISTRIBUTIONS ALONG BODIES OF PARABOLIC THICKNESS DISTRIBUTION $\left(\text{NOSE RADIUS} = 9\,t_0^2/32\,L\right)$
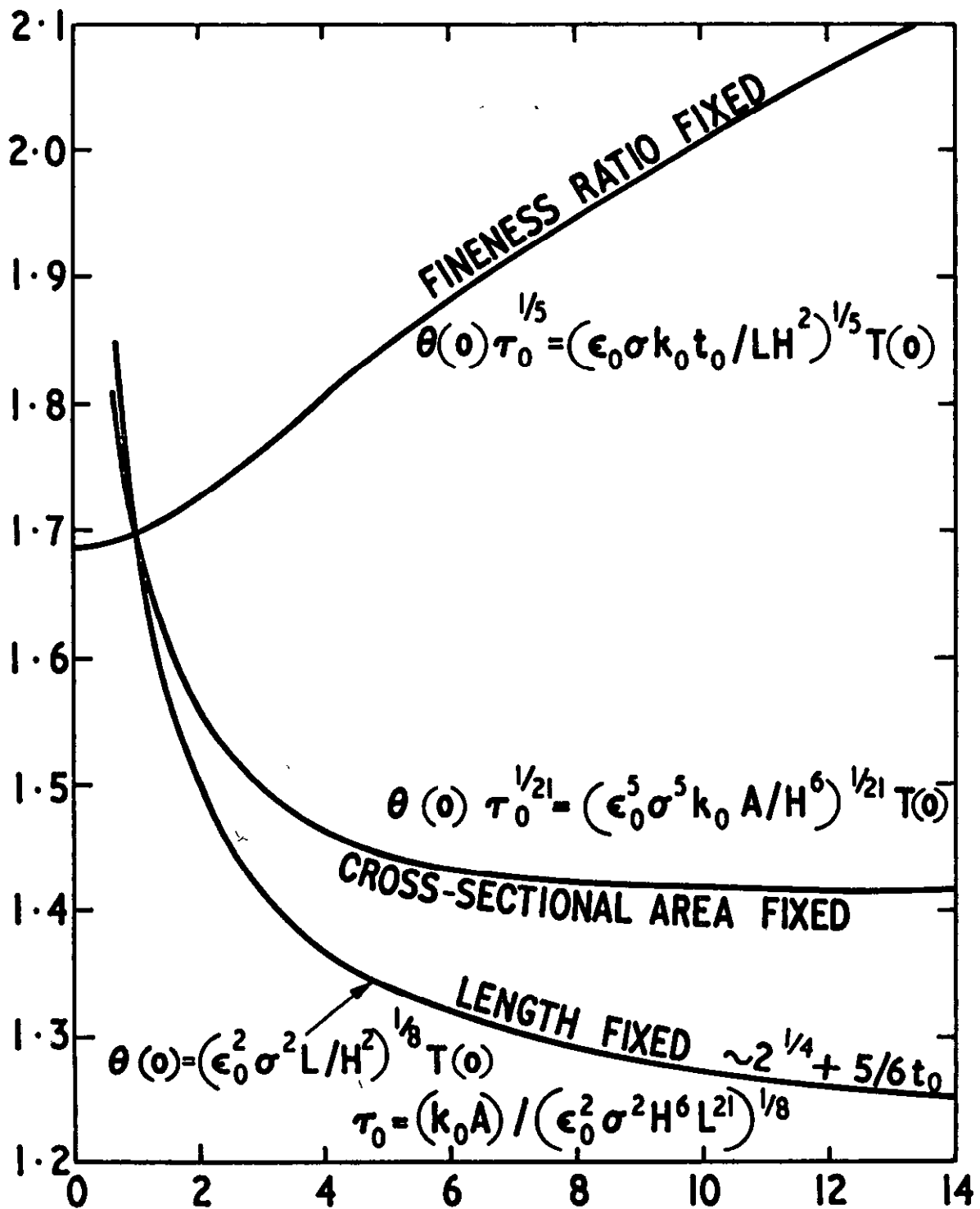
Fig. 7. NOSE TEMPERATURE FOR WEDGE SHAPED THICKNESS DISTRIBUTIONS.

$$\theta(1) = \left(\epsilon_0^2 \sigma^2 L / H^2\right)^{1/8} T(L) = T(L)/T_0$$

$$\tau_0 = \left(k_0 A\right) / \left(\epsilon_0^2 \sigma^2 H^6 L^{21}\right)^{1/8}$$
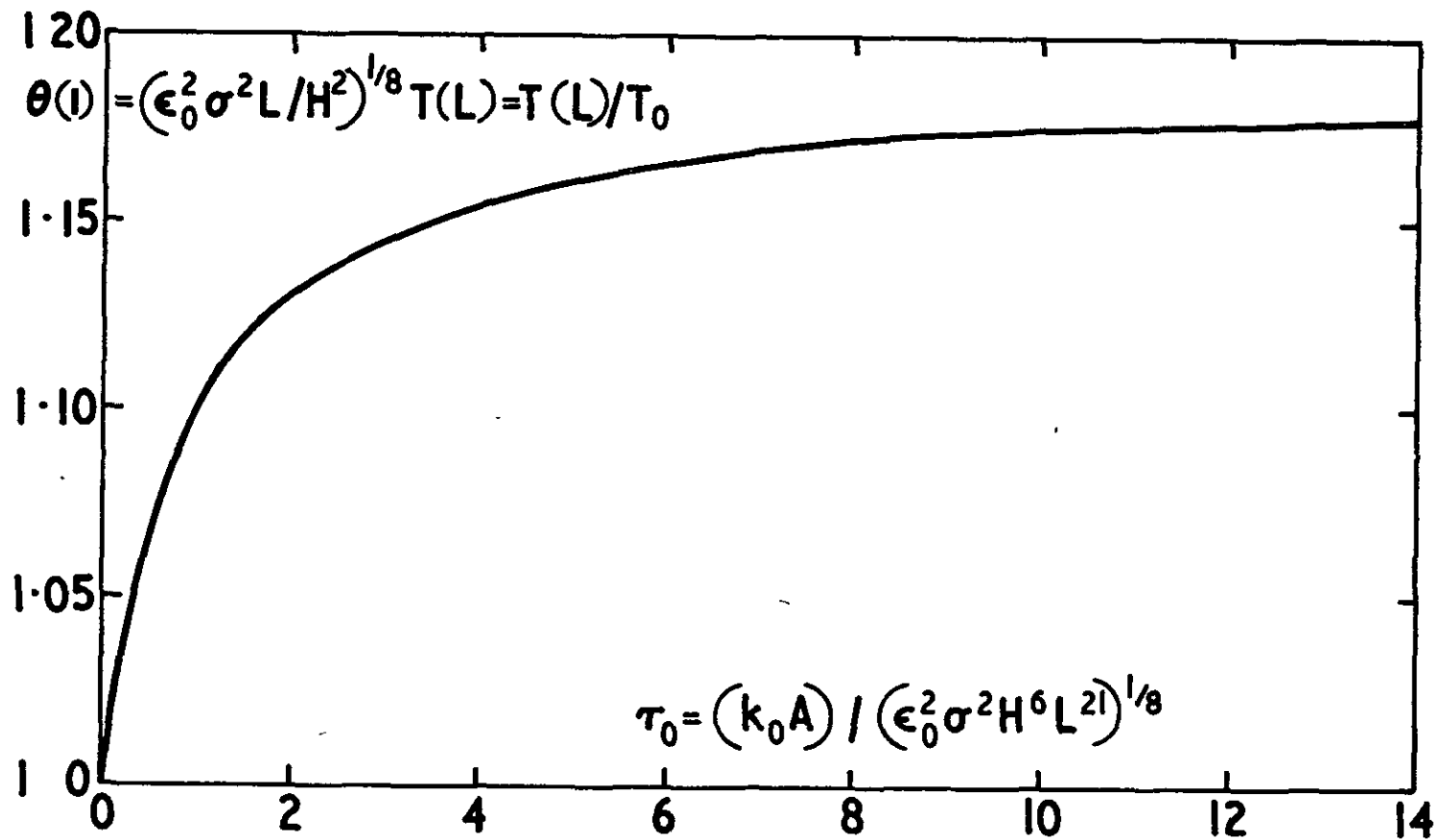
Fig. 8   RATIO OF TEMPERATURE TO RADIATION EQUILIBRIUM
TEMPERATURE AT REAR OF WEDGE-SHAPED BODY.
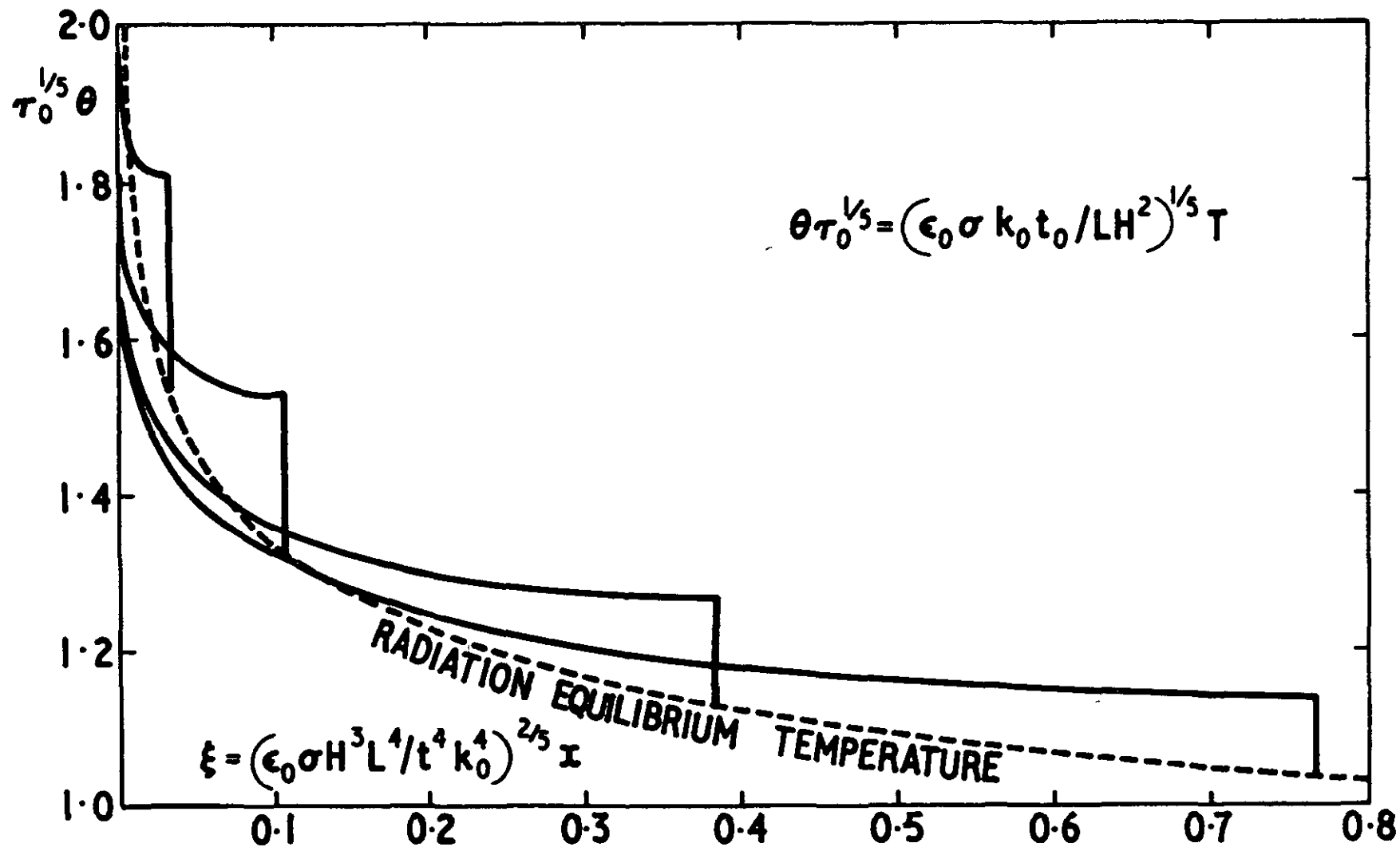
Fig. 9. SOME TEMPERATURE DISTRIBUTIONS ON WEDGE-SHAPED BODIES.
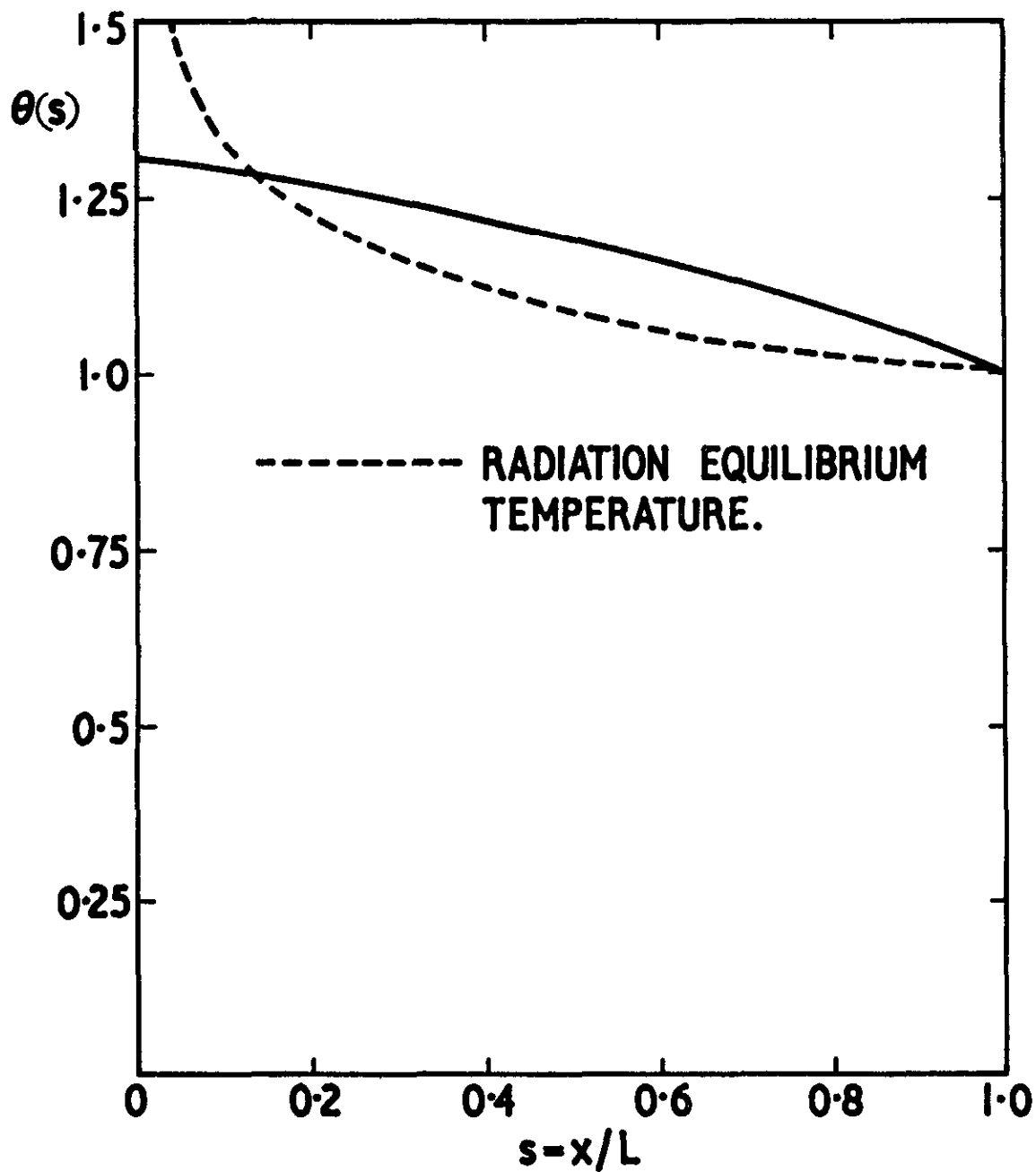
Fig. IO. TEMPERATURE DISTRIBUTION OVER SHAPE HAVING MINIMUM CROSS-SECTIONAL AREA FOR STIPULATED NOSE TEMPERATURE.

OPTIMAL DISTRIBUTION

 A = 1

UNIFORM TEMPERATURE GRADIENT

 A = 1·05

UNIFORM THICKNESS

 A = 1·45
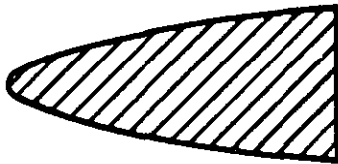
 PARABOLA A = 2·35
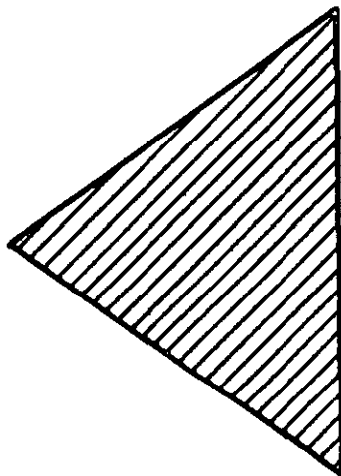
 WEDGE A = 6·9

Fig. 11. OPTIMISED SHAPES PROVIDING SAME NOSE TEMPERATURE. (THICKNESS & LENGTH SCALES COMMON BUT UNDEFINED.)
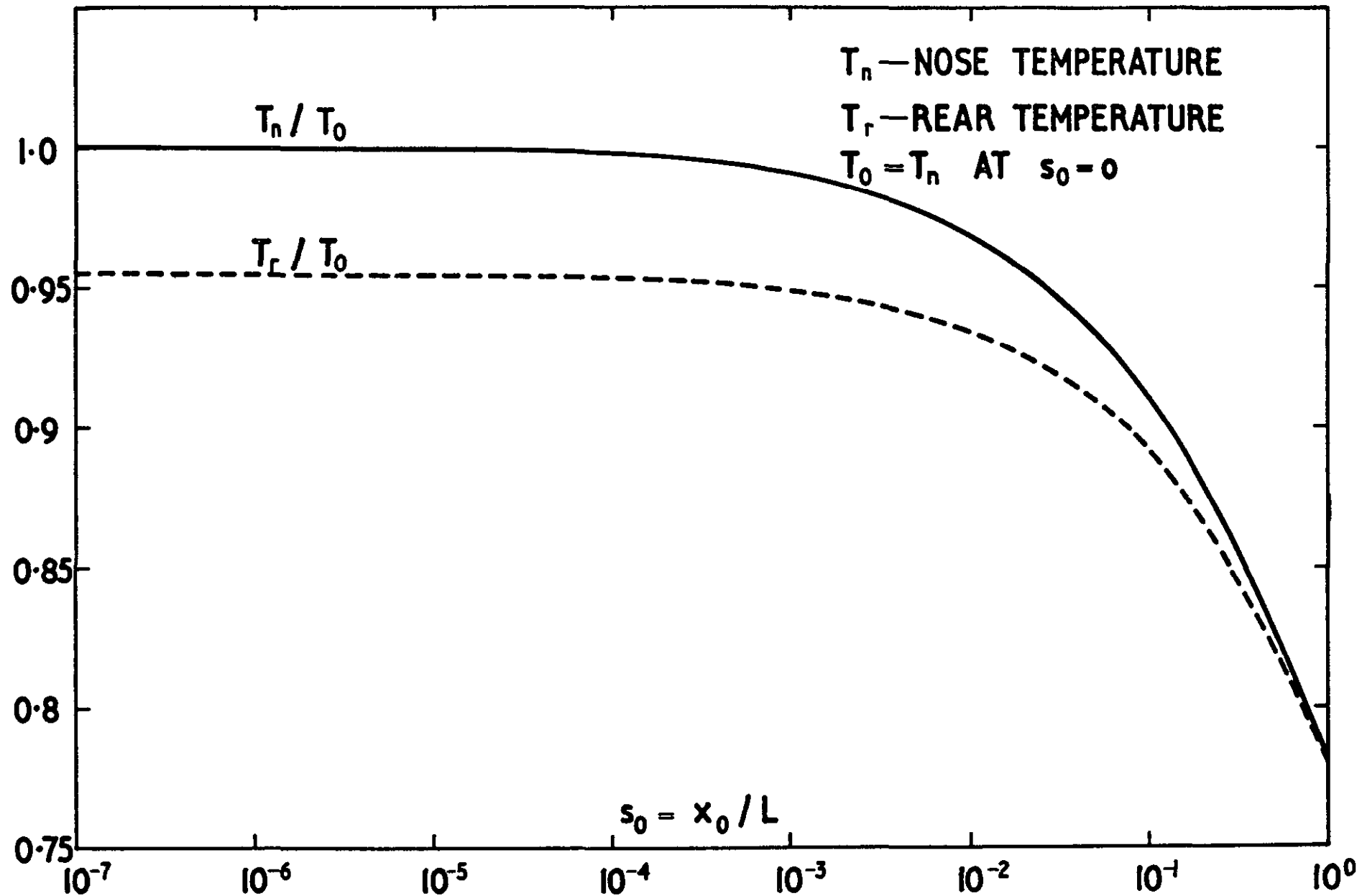
Fig.12. EFFECT OF s_0 ON NOSE AND REAR TEMPERATURE.
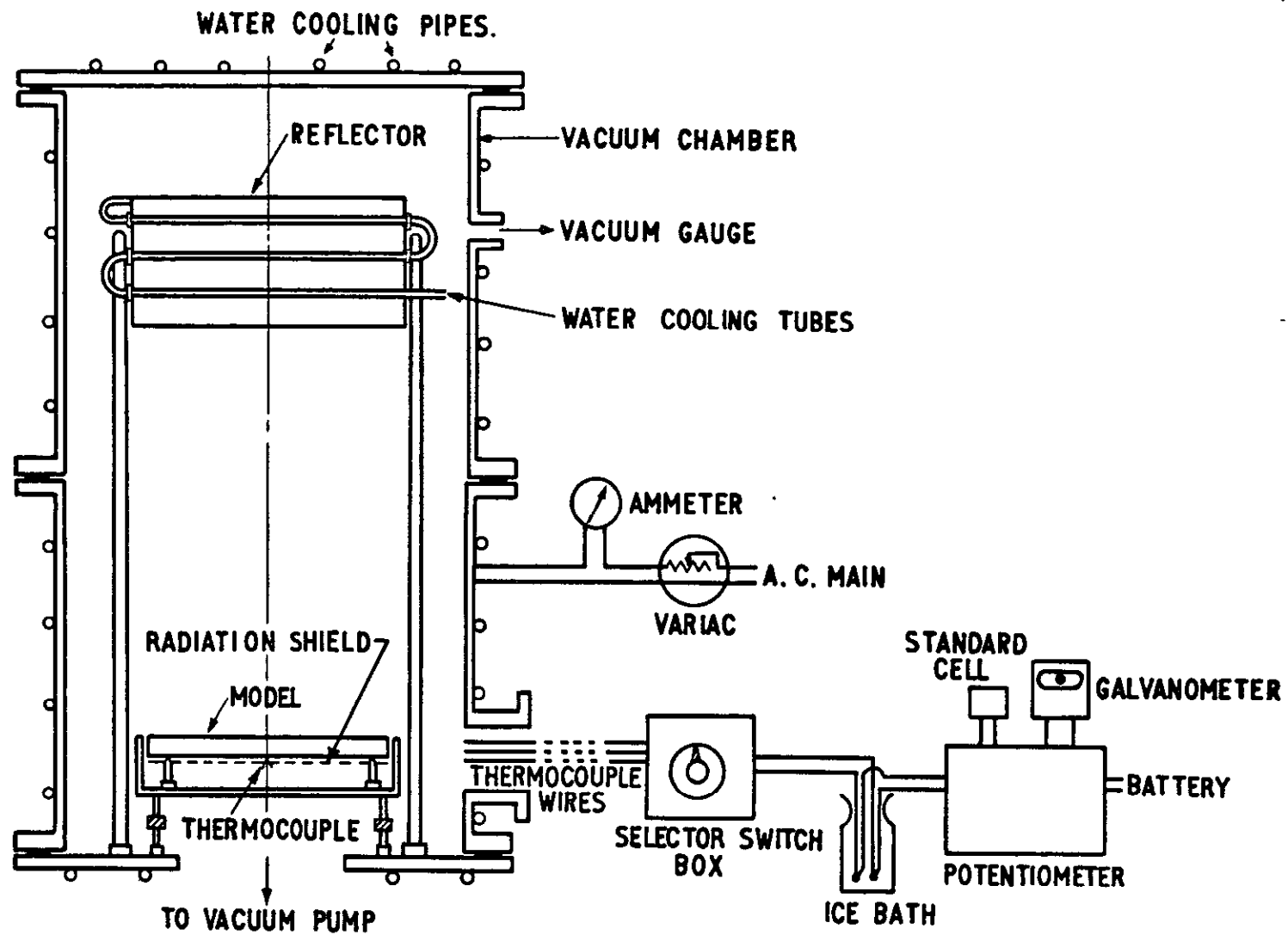
GENERAL LAYOUT OF APPARATUS

Fig. 13.
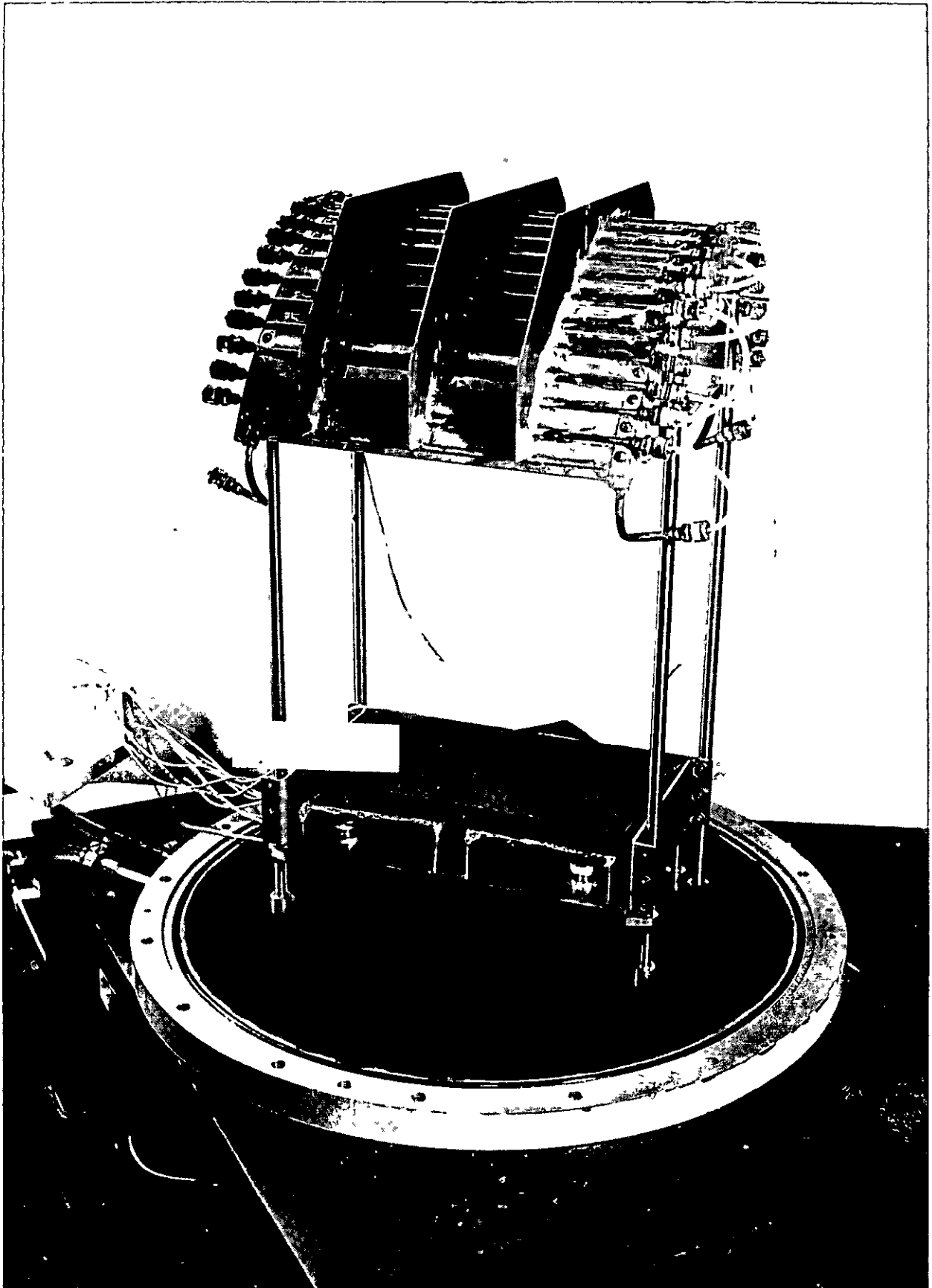
Fig. 14   General arrangement of model and reflector.
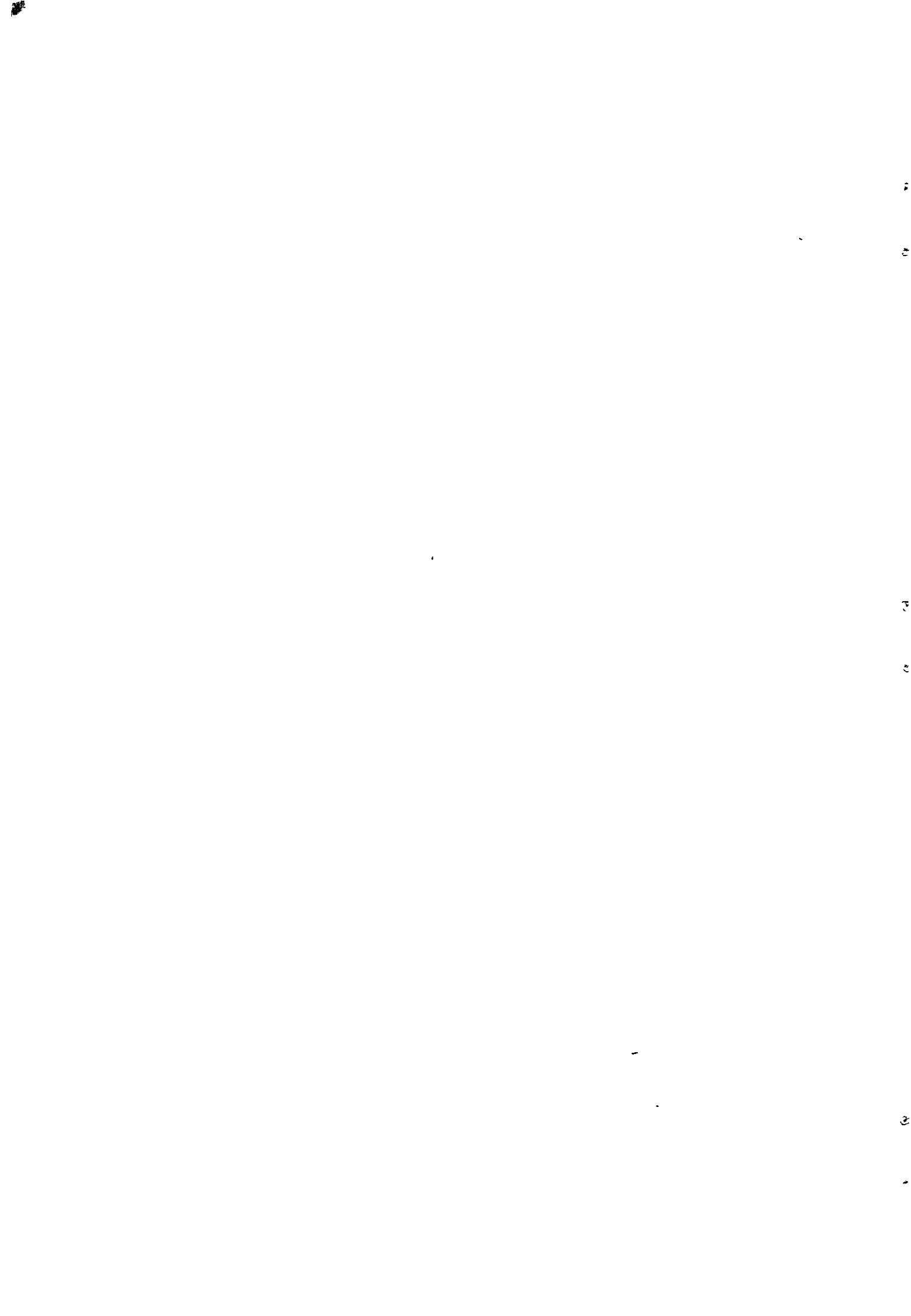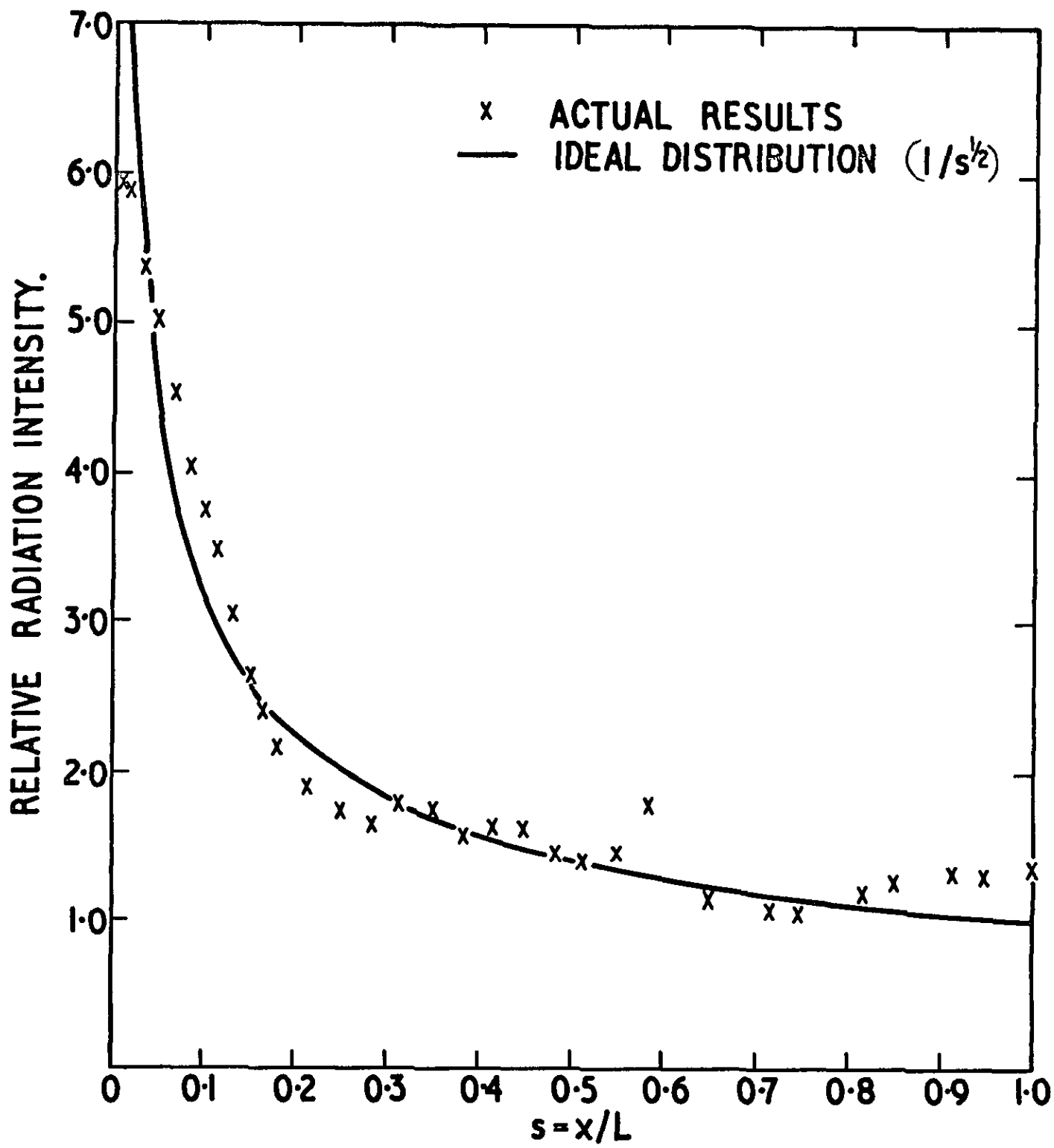
Fig.15. PERFORMANCE OF REFLECTOR.
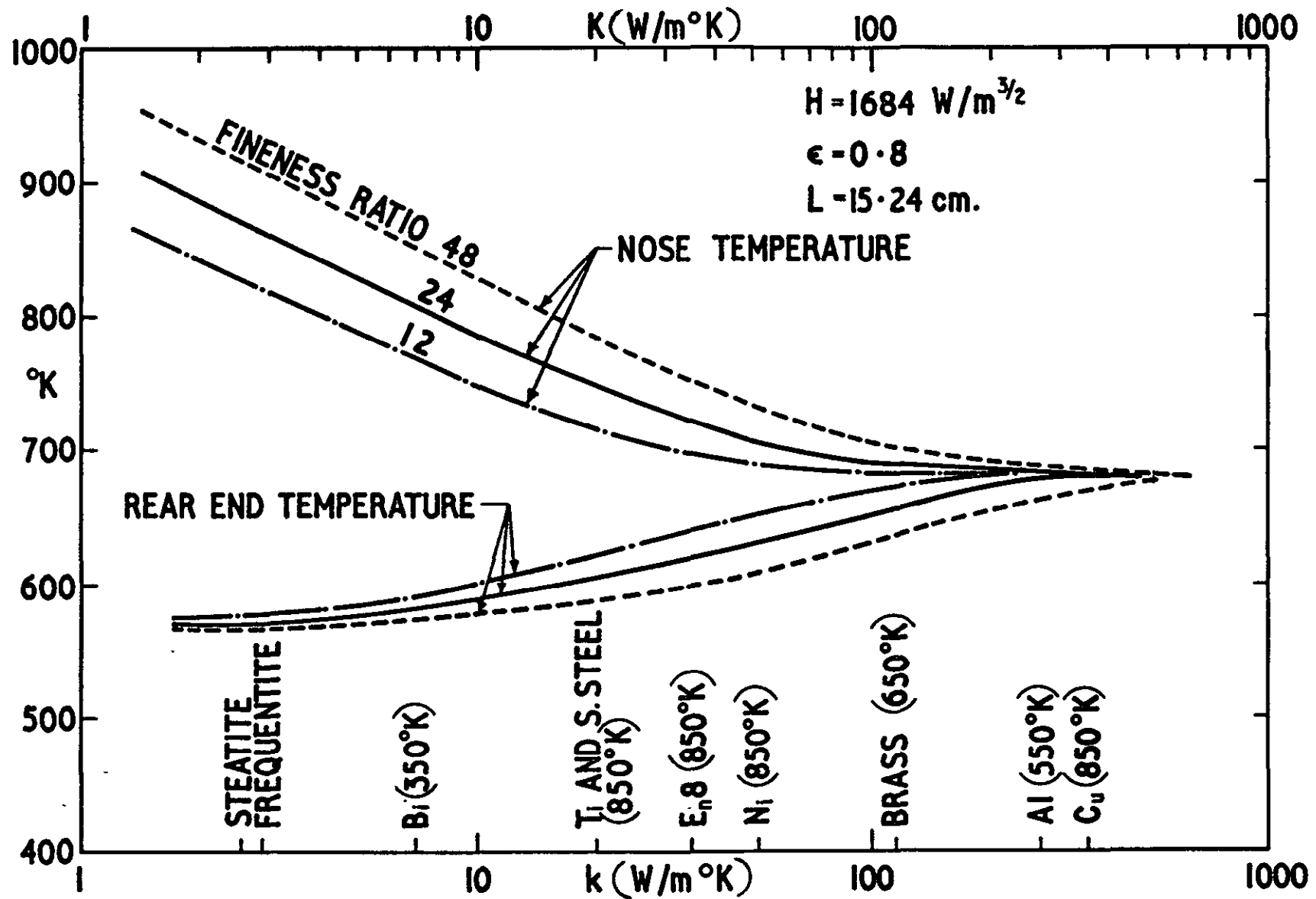
Fig.16. EFFECT OF THERMAL CONDUCTIVITY ON NOSE AND REAR END TEMPERATURES.
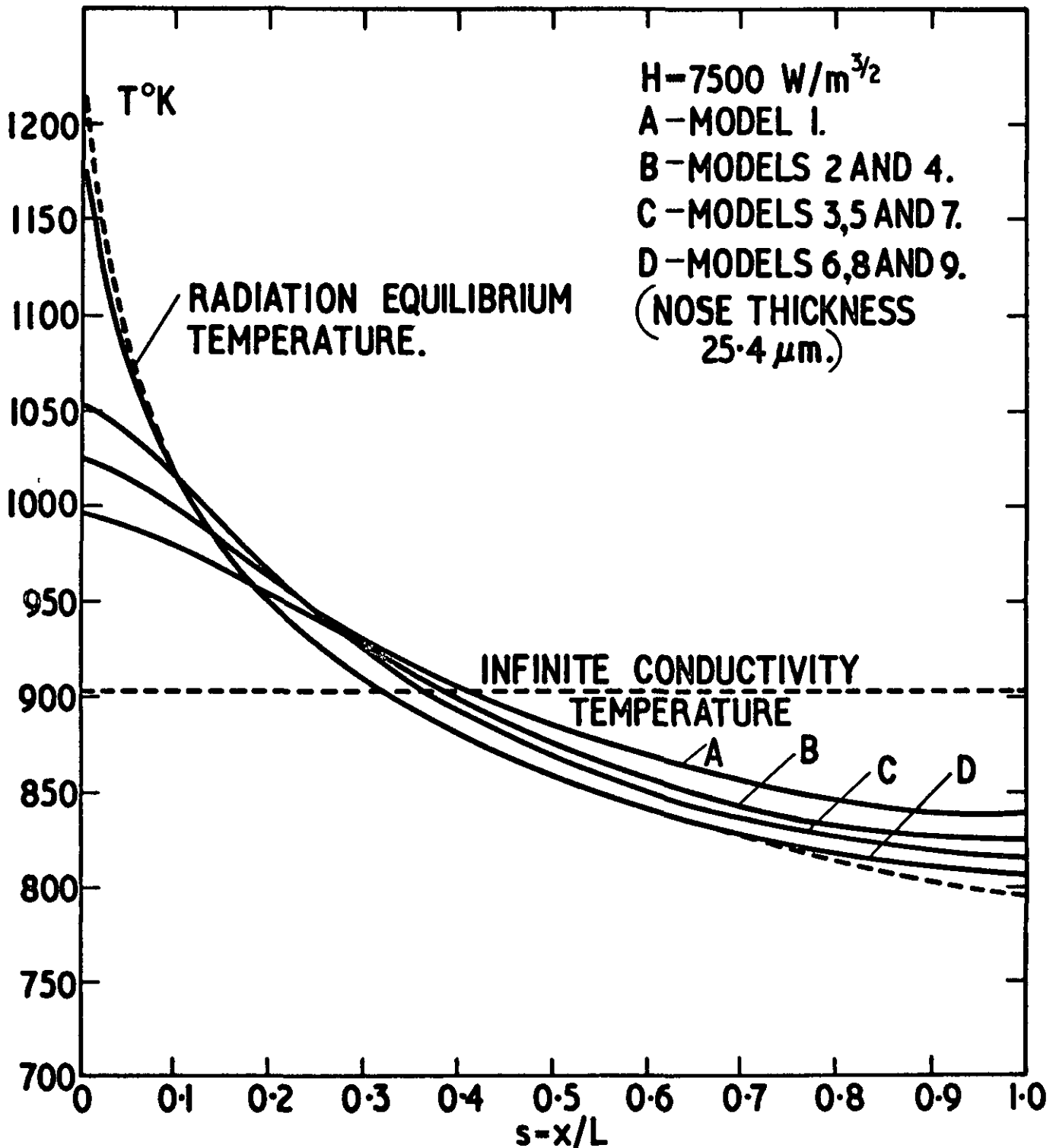
Fig.17. COMPUTED TEMPERATURE DISTRIBUTION IN MODELS SUBJECT TO A GIVEN HEAT INPUT.
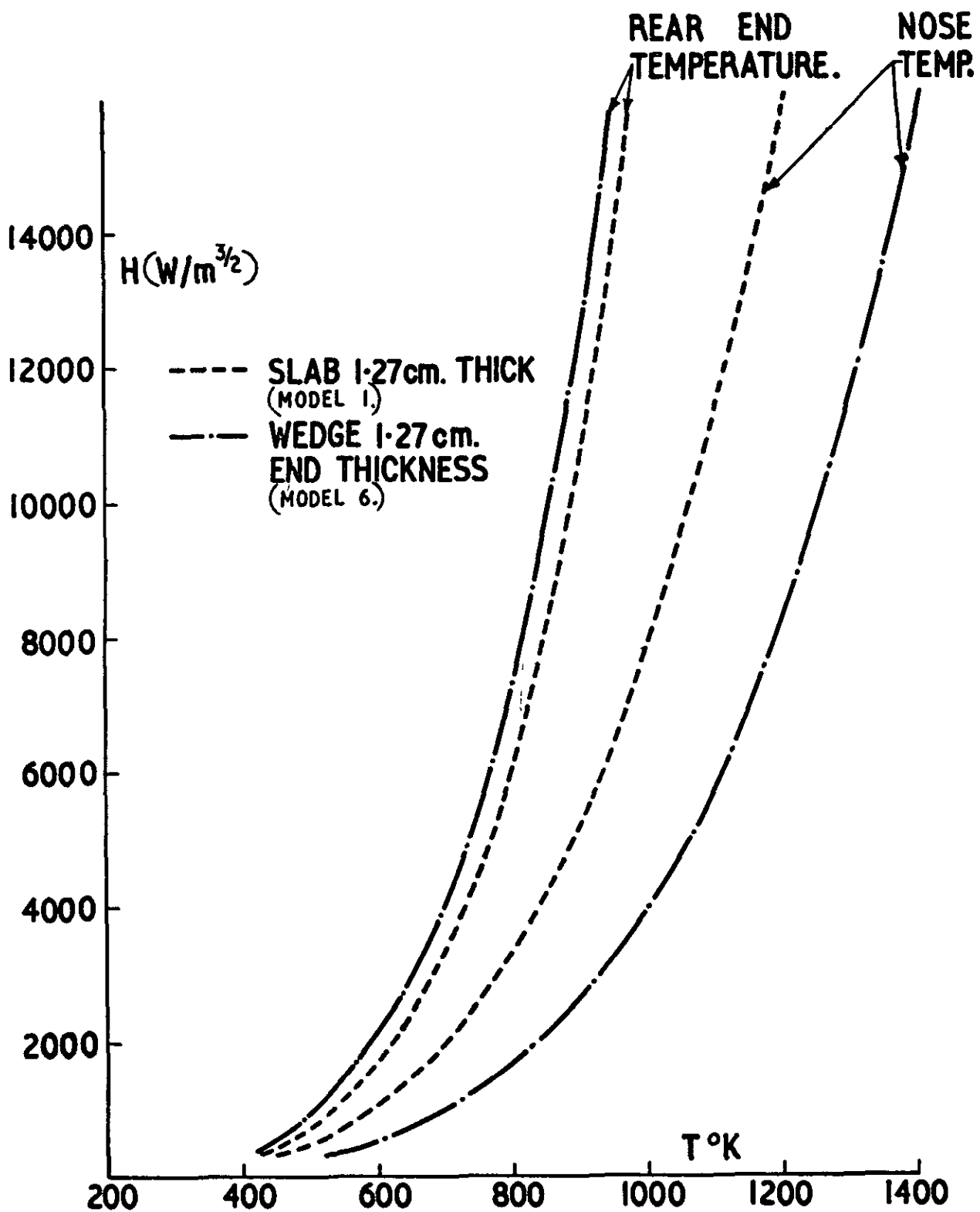
Fig. 18. EFFECT OF HEAT INPUT ON NOSE AND REAR END TEMPERATURE OF SLAB AND WEDGE MODELS.

Fig. 19

MODEL 1
SLAB 1·27 cm THICK
$H = 1179$ watts$/m^{3/2}$
x EXPERIMENT
— THEORY

$T°K$

$s = x/L$

Fig. 20

MODEL 2
SLAB 0·635 cm THICK
$H = 1165$ watts$/m^{3/2}$
x EXPERIMENT
— THEORY

$T°K$

$s = x/L$

Fig. 21.

MODEL 3.
SLAB 0·317cm. THICK
H = 1281 watts/m$^{3/2}$
× EXPERIMENT
— THEORY

T°K

s = x/L

Fig. 22.

MODEL 4.
TRAPEZOIDAL 0·635cm.–1·27cm.
H = 1220 watts/m$^{3/2}$
× EXPERIMENT
— THEORY

T°K

s = x/L

Fig. 23

MODEL 5
TRAPEZOIDAL 0·317 cm – 1·27 cm
$H = 1167$ watts /m$^{3/2}$
x EXPERIMENT
— THEORY

$T°K$

$s = x/L$

Fig. 24

MODEL 6
WEDGE SECTION, 1·27 cm END THICKNESS
$H = 1192$ watts /m$^{3/2}$
x EXPERIMENT
— THEORY

$T°K$

$s = x/L$

Fig. 25.

MODEL 7.
TRAPEZOIDAL 0·317 cm.–0·635 cm
H = 1266 watts/m$^{3/2}$
x EXPERIMENT
— THEORY

$s = x/L$

Fig. 26.

MODEL 8.
WEDGE SECTION 0·635 cm.
END THICKNESS.
H = 1228 watts/m$^{3/2}$
x EXPERIMENT
— THEORY

$s = x/L$

Fig. 27.

MODEL 9.
WEDGE SECTION 0·317cm.
END THICKNESS.
$H = 1190$ watts/$m^{3/2}$
x   EXPERIMENT
— THEORY

$T°K$

$s = x/L$

Fig. 28.

MODEL 10
SLAB 1·27 cm. THICK
H = 440 W/m$^{3/2}$
x EXPERIMENT
— THEORY

T°K

s = x/L

Fig. 28.

MODEL 10
SLAB 1·27 cm. THICK
H = 631 W/m$^{3/2}$
x EXPERIMENT
— THEORY

T°K

s = x/L

NOSE OF MODEL

CENTRE SECTION

REAR END OF MODEL

d

a

b

L

X   THERMOCOUPLE POSITION.

Fig. 29.   TEST MODEL.

and the results thus obtained are compared with those
predicted by the theory.

and the results thus obtained are compared with those
predicted by the theory.

and the results thus obtained are compared with those
predicted by the theory.

A.R.C. C.P. No.1126
June, 1969
Nonweiler, T., Wong, H. Y. and Aggarwal, S. R.

THE ROLE OF HEAT CONDUCTION IN LEADING EDGE HEATING
THEORY AND EXPERIMENT

The effect of heat conduction of material on the
temperature distribution in the vicinity of a wing
leading edge in hypersonic flight is investigated. The
theory is based on a conducting plate subjected to
aerodynamic heating. It is found that the role played by
the conductivity of the material and the leading edge
thickness in moderating the nose temperature is very
significant. Detailed discussions of the numerical
solutions for various shapes of leading edge are given.
An experimental technique has been developed by which a
number of models representing a wing leading edge can be
tested/